

**RL-TR-96-61**  
**Final Technical Report**  
**May 1996**



# **SEMICONDUCTOR RING LASERS**

**Cornell University**

**Sponsored by**  
**Advanced Research Projects Agency**

*APPROVED FOR PUBLIC RELEASE; DISTRIBUTION UNLIMITED.*

The views and conclusions contained in this document are those of the authors and should not be interpreted as necessarily representing the official policies, either expressed or implied, of the Advanced Research Projects Agency or the U.S. Government.

**19960910 068**

**DTIC QUALITY INSPECTED 3**

**Rome Laboratory**  
**Air Force Materiel Command**  
**Rome, New York**

UNCLASSIFIED  
Technical Report  
Available by

**DEFENSE  
TECHNICAL  
INFORMATION  
CENTER**

DTIC / Acquiring Information - Inspiring Creativity

**DEFENSE LIBRARY  
CONNECTION**  
Alexandria, Virginia 22304-6144

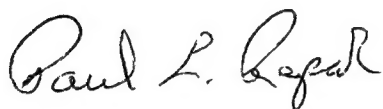
UNCLASSIFIED

**THIS DOCUMENT IS BEST  
QUALITY AVAILABLE. THE COPY  
FURNISHED TO DTIC CONTAINED  
A SIGNIFICANT NUMBER OF  
PAGES WHICH DO NOT  
REPRODUCE LEGIBLY.**

This report has been reviewed by the Rome Laboratory Public Affairs Office (PA) and is releasable to the National Technical Information Service (NTIS). At NTIS, it will be releasable to the general public, including foreign nations.

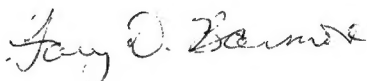
RL-TR- 96-61 has been reviewed and is approved for publication.

APPROVED:



PAUL L. REPAK  
Project Engineer

FOR THE COMMANDER:



GARY D. BARMORE, Major, USAF  
Deputy Director of Surveillance & Photonics

If your address has changed or if you wish to be removed from the Rome Laboratory mailing list, or if the addressee is no longer employed by your organization, please notify Rome Laboratory/ ( OCPC ), Rome NY 13441. This will assist us in maintaining a current mailing list.

Do not return copies of this report unless contractual obligations or notices on a specific document require that it be returned.

SEMICONDUCTOR RING LASERS

J.M. Ballantyne

Contractor: Cornell University  
Contract Number: F30602-92-C-0082  
Effective Date of Contract: 27 July 1992  
Contract Expiration Date: 31 October 1995  
Short Title of Work: Semiconductor Ring Lasers

Period of Work Covered: 7/92 - 10/95

Principal Investigator: J.M. Ballantyne  
Phone: (607) 255-5014

RL Project Engineer: Paul L. Repak  
Phone: (315) 330-3146

Approved for public release; distribution unlimited.

This research was supported by the Advanced Research Projects Agency of the Department of Defense and was monitored by Paul L. Repak, Rome Laboratory/OCPC, 25 Electronic Pky, Rome NY 13441-4515.

# REPORT DOCUMENTATION PAGE

Form Approved  
OMB No. 0704-0188

Public reporting burden for this collection of information is estimated to average 1 hour per response, including the time for reviewing instructions, searching existing data sources, gathering and maintaining the data needed, and completing and reviewing the collection of information. Send comments regarding this burden estimate or any other aspect of this collection of information, including suggestions for reducing this burden, to Washington Headquarters Services, Directorate for Information Operations and Reports, 1215 Jefferson Davis Highway, Suite 1204, Arlington, VA 22202-4302, and to the Office of Management and Budget, Paperwork Reduction Project (0704-0188), Washington, DC 20503.

1. AGENCY USE ONLY (Leave Blank)		2. REPORT DATE May 1996		3. REPORT TYPE AND DATES COVERED Final Jul 92 - Oct 95	
4. TITLE AND SUBTITLE  SEMICONDUCTOR RING LASERS				5. FUNDING NUMBERS C - F30602-92-C-0082 PE - 61101E/62702F PR - H682 TA - 00 WU - 01	
6. AUTHOR(S)  J.M. Ballantyne					
7. PERFORMING ORGANIZATION NAME(S) AND ADDRESS(ES) Cornell University Office of Sponsored Programs 120 Day Hall Ithaca NY 14853-5401				8. PERFORMING ORGANIZATION REPORT NUMBER  N/A	
9. SPONSORING/MONITORING AGENCY NAME(S) AND ADDRESS(ES) Advanced Research Projects Agency 3701 North Fairfax Drive      Rome Laboratory/OCPC Arlington VA 22203-1714      25 Electronic Pky Rome NY 13441-4515				10. SPONSORING/MONITORING AGENCY REPORT NUMBER  RL-TR-96-61	
11. SUPPLEMENTARY NOTES  Rome Laboratory Project Engineer: Paul L. Repak/OCPC/(315) 330-3143					
12a. DISTRIBUTION/AVAILABILITY STATEMENT  Approved for public release; distribution unlimited.				12b. DISTRIBUTION CODE	
13. ABSTRACT (Maximum 200 words)  This program investigated the potential performance of triangular, monolithic, waveguide diode ring lasers (WDRL) for applications in high power, low-noise, short-to-medium-distance data transmission. This project illuminated many fascinating features of the physics of these devices, and has resulted in new methods for achieving unidirectionality in ring lasers. High power (10-20 mW), low-noise (-150 to -170 dBm) lasers appear feasible and provide low cost manufacturability and integrability. WDRLs integrated with small amplifiers showed 85 mW single mode outputs. Because these WDRLs are the first traveling wave lasers to operate entirely in single mode waveguide, they show a combination of attractive features not found in other lasers. Records include the first development of a nonreciprocal reflector concept and model for unidirectional ring lasers; high quality etched turning mirrors; record low threshold single mode ring lasers; record high ring laser external efficiency; and record high ring laser output power.					
14. SUBJECT TERMS  Semiconductor lasers, Electrooptics				15. NUMBER OF PAGES 114	
				16. PRICE CODE	
17. SECURITY CLASSIFICATION OF REPORT UNCLASSIFIED	18. SECURITY CLASSIFICATION OF THIS PAGE UNCLASSIFIED	19. SECURITY CLASSIFICATION OF ABSTRACT UNCLASSIFIED	20. LIMITATION OF ABSTRACT UL		

## INDEX

	page
1. Introduction	3
Work Schedule	4
2. Accomplishments	5
Modeling/Simulation	5
Advanced Fabrication Processes	7
Unidirectional WDRLs	7
Longer Wavelength WDRLs	8
Record Performance WDRLs	9
Noise Properties	10
WDRL Arrays and Integration	15
3. Summary and Outlook	16
4. Publications List	18
5. List of Personnel	20
Graduate Degrees	20
Appendix 1	21
References	25
Appendix 2	26
Appendix 3	40
Appendix 4	72
Appendix 5	85
Appendix 6	95

## 1. Introduction

A major bottleneck in very high speed information acquisition and processing systems is the rate of data communication within the system. As data rates increase on electrical busses, so does the power required to send the data and problems of cross talk and noise become more severe. These problems can be eliminated by using photons, instead of electrons, to transfer data from one point to another within the system. However, major limitations of current photonics data transmission components include the lack of easily integrable lasers and the noise level in the transmitter. For high rate analog data transmission, the noise level of the transmitter is especially critical. There is therefore a great need for small, integrable, very low noise, efficient optical sources for transmitting data at microwave and millimeter wave rates over relatively short distances.

One characteristic of most applications for short distance optical interconnects is the highly parallel nature of such interconnects which requires many transmitters and receivers. One of the most significant problems is the conversion of electrical to optical signals in a way which is efficient and compatible with silicon chip technology in terms of manufacturability, cost per function, size, reliability, and power density. In the current decade we invented and demonstrated a new class of semiconductor lasers which has the potential to meet all of these requirements and in addition will likely have extremely low relative intensity noise levels. These devices are monolithic guided-wave diode ring lasers which we dub Waveguide Diode Ring Lasers (WDRL) for brevity. Unique properties of these devices, which include the ability to operate as unidirectional traveling wave oscillators and hence promise extremely low noise and sensitivity to reflections, are a consequence of the fact that these are the first ring lasers to be completely constructed in low-order dielectric waveguides. In addition, these devices are unique in that they allow laser resonant cavities of engineerable high  $Q$  to be constructed using a highly manufacturable technology: chemically assisted ion beam etching (CAIBE); these cavities can be placed anywhere and in any orientation on a wafer, and these are the only diode ring lasers to contain a simple, variable output coupling mechanism as an intrinsic part of the cavity.

These laser geometries have the potential to produce a small, low threshold, monolithically integrated device which can be easily coupled to planar waveguides and which does not require special facet coatings for high reflectivity. The basic configuration is a planar, triangular-ring, single mode, rib waveguide. Since all reflections can be total internal ones, the optical cavity can be high- $Q$ , allowing for very low threshold current operation. These unique properties of manufacturability, integrability, adjustable  $Q$  with planar cavity, built in output coupler, non-reciprocal operation, and ultra-low noise make this a unique class of devices which are important for future study.

The major objective of the work reported here was to gain a more complete understanding of the physics of the operation of these devices from both a theoretical and experimental approach, so as to determine the performance limits of such structures. The work proposed for this study included theoretical modeling, comparison of the models with experimental results on actual devices, the

development of design tools for producing high-power and low noise ring lasers, and the development of the lowest possible noise, high-power, monolithic ring laser for analog communication applications. While most of the work was to be done using the GaAs based material system, the program was also to contain a component to develop the materials technology to produce monolithic ring lasers at 1.3 micron wavelengths on InP substrates. It was also to include an investigation of the properties of arrays of monolithic ring lasers and the coupling of such ring lasers to planar optical waveguides. The final objective was to produce diode ring lasers with power output of 50 to 100 milliwatts and relative intensity noise less than -160 dB, together with the ground work necessary to produce arrays of such devices operating at 1.3 micron wave lengths. The milestone list from the original proposal follows. As will be seen from the next section, nearly all of the original goals and milestones were actually achieved. The state of understanding and performance of WDRs prior to the work done on this contract is summarized in Appendix 1, Technical Background, which is an abridgement of a section from the original proposal.

## **Work Schedule**

### **Year 1**

- Model unidirectional DRL; complete eigenmode cavity analysis.
- First results of finite element cavity analysis.
- Fabricate and test unidirectional DRLs with various assymetries; compare results with model.
- Measure intensity noise and cavity Q of DRLs.
- Complete 1.3  $\mu\text{m}$  MOCVD growth system.
- Select 1.3  $\mu\text{m}$  MOCVD materials system; Grow and characterize quaternary materials for 1.3  $\mu\text{m}$  DRLs.
- Preliminary development of CAIBE processing technique for 1.3  $\mu\text{m}$  materials.

### **Year 2**

- Develop design tools for cavity Q vs geometry.
- Design long cavity, weak guide DRLs for lowest noise.
- Design waveguide output coupler; extend analysis with two-dimensional transforms.
- Complete finite-element cavity analysis
- Fabricate and test low-noise DRLs.
- Fabricate and test DRL linear arrays.
- Fabricate and test DRLs with integrated waveguide output.
- Complete development of CAIBE process for 1.3  $\mu\text{m}$  DRL.
- Grow and characterize 1.3  $\mu\text{m}$  quaternary GRINSCH structures.



### Year 3

- Develop design tools for optimized low-noise, high power DRL.
- Fabricate and test low-noise, high power DRLs.
- Fabricate and test lowest-noise DRL.
- Fabricate and test lowest-noise DRL integrated with output amplifier, if necessary.
- Fabricate and test 1.3  $\mu\text{m}$  DRLs.
- Develop a 1.3  $\mu\text{m}$  pseudomorphic QW materials system for DRLs.

## 2. Accomplishments

Nearly all of the original goals and milestones for this work were actually accomplished. All of the theoretical predictions and experimental measurements are consistent in supporting the original conjectures on the promise of WDRLs. We have shown that these devices provide a unique combination of features unmatched by any other laser, including: low-cost, high volume manufacturability; very high spectral purity, sidemode suppression, and low noise; unidirectional traveling wave operation which obviates the need for optical isolators; easy monolithic integration with amplifiers and waveguides; relatively high output power; good efficiency, and very small physical size. It should be emphasized that the last three features are a consequence of the triangular geometry, and are not common to other forms of monolithic diode ring lasers such as squares or ovals.

Our accomplishments can be grouped in the following categories

- Development of a modeling/simulation tool suite which includes 3D dielectric mirror analysis, laser eigenmode analysis, geometry optimization, and finite element modeling.
- Development of advanced self-aligned fabrication processes which result in high-quality, repeatable optical cavity formation for large numbers of lasers/ waveguides/amplifiers/detectors, etc.
- Development of new physical principles and techniques for producing unidirectional WDRLs.
- Development of materials and fabrication technology for longer wavelength (1.3  $\mu\text{m}$ ) WDRLs.
- Use of all of the above to fabricate devices which set performance records for diode ring lasers.

Specific accomplishments in each category are listed and discussed below.

### Modeling/Simulation

We completed the first fully 3-D analysis of a turning mirror of arbitrary angle and geometry which couples two dielectric waveguides (in our case ridge waveguides). (cf publications 8 and 9) This was a very significant development which

provided for the first time realistic coupling and loss computations of dielectric waveguides coupled by planar turning mirrors. The 3-D analysis gives significantly different coupling and loss values than any prior modelings, including our own previous 2-D analysis which was the first to treat the general case (publications 1 and 3). Major conclusions are 1) a limit on the highest cavity Q attainable for any geometry, 2) provision of a tool for predicting cavity Q and device properties vs. geometry, 3) prediction of a unique crescent-shaped far field, which was experimentally confirmed, 4) provision of a tool for computing coupling efficiencies of lasers and waveguides, 5) prediction of the losses arising from variations in ideality of mirror geometry due to process variations, 6) provision of a tool for optimizing device geometries including waveguide design, 7) provision of a tool for calculating scattering matrix parameters. This work showed that efficient turning mirrors can be constructed in a small space which allow small, low threshold WDRLs to be built.

The laser eigenmode analysis (publications 2 and 6) is very significant because it is the first tool which can take the complex scattering matrix coefficients calculated by the preceding 3-D mirror analysis and predict the laser eigenmodes. Hence the longitudinal mode spacing, and more importantly, the degree of unidirectionality of the device can be predicted. Using the latter feature, we have determined that unidirectionality is a very sensitive function of any asymmetry in either forward or reflection scattering matrix parameters (in either amplitude or phase). This result led directly to our discovery of new methods for making unidirectional ring lasers, discussed later.

Coupling the two preceding analyses together, we now have a means to optimize WDRL geometries as a whole for parameters such as threshold current, power output, output beam shape. For the first two quantities we must also consider properties of the gain medium in the device. Using parameters for the gain medium from our own, and other's measurements, we have determined for example (for a related contract) that a WDRL constructed in pseudomorphic GaInAs/GaAs material with  $30^\circ$  structure angle, and  $100\mu$  total length should lase with threshold current under 2 ma. This device will fit in a triangle with  $30\mu$  base and  $35\mu$  height, and is an excellent candidate to replace electrical output pads in ULSI chips around the year 2007. The device size is considerably smaller than the  $50 \times 50\mu^2$  area projected for that generation, and will consume far less power and operate much faster than an electrical output. This application is being pursued under a separate, SRC-sponsored program.

The models discussed above use a spatial Fourier-transform approach to expand the actual mode shapes and propagate them through the structure. They are thus incapable of dealing with the sharp geometrical features of our structures and issues such as tunneling between the guides where they join. Therefore they cannot be used to model the optical diodes which we use in unidirectional devices. To handle these issues we have also pursued finite element, or boundary element approaches to directly solve Maxwell's equations in our structures. We have made substantial progress, but not completed this work, which is ongoing. S. Lau developed automatic gridding software for our geometry, and Dr. Simon Gdzelishvili spent 9 months with us developing a

boundary-element solution to our problem. He coded his solution for a trial case, but had to leave before the code was debugged. The work continues. Both of these approaches were for 2-D structures. A 2-D approach can give us insight, but will not provide quantitative modeling. We recently located 3-D finite element code from a commercial vendor which appears capable of solving our problems. However, the 3-D problem is huge, and requires a supercomputer. In cooperation with the vendor, we are now developing this application on the National Supercomputer Center at Cornell, and anticipate results in a few months. This will allow us to compute scattering matrices for optical diodes and to predict a priori the properties of unidirectional WDRLs.

### Advanced Fabrication Processes

The WDRL is a highly-manufacturable, cheap, device because it is fabricated using planar, batch processing like MOS chips. Process steps include photolithography, dry etching and thin film deposition. We pioneered the use of etching processes for diode laser optical cavities and have refined the process over the years. Under this program we have further refined the technology so that we now produce the world's best etched mirrors. We achieve reflective coupling efficiency exceeding 88% for a rather tight transverse confinement in ridge waveguides—a record.

Another key element was the development in this work of a self-aligned process for producing WDRLs combining perfect alignment with excellent mirrors. This process is described in publications 5 and 12. It is key to obtaining reproducible, ideally symmetric far fields like that shown in Fig. 4 of Appendix 2. It is also key to obtaining controllable unidirectional operation as described in Appendix 4. An important element of this process is the single-step etching of the deep mirrors self-aligned to the previously shallow-etched rib.

### Unidirectional WDRLs

For the reasons described in Appendix 1, unidirectionality is a key element of high-performance WDRLs. The uniform longitudinal photon density in a traveling-wave provides a single, spectrally narrow, output mode with very high side-mode suppression (we measure  $>25$  db: cf Fig. 5, Appendix 4) and lower noise (discussed later and in Appendix 1). It also results in a single output beam. We have measured single-beam slope efficiency of 0.23 W/A, about an order of magnitude higher than any other diode ring laser.

Most importantly, we have developed both the theory and practice of a new method for making unidirectional ring lasers. This is based on the concept of a nonreciprocal reflector (described in Appendix 6) where we demonstrate the principle in a simple, closed-form solution. Waveguide implementation via an "optical diode" or tapered leg is shown in Figs. 1 and 2 of Appendix 4. These concepts are covered in a patent application. They result in forward/backward beam ratios of 20:1 (optical diode) or 30:1 (tapered leg), with the former showing almost no increase in loss in the cavity (as shown by a less than 5% increase in

threshold current for unidirectional vs bidirectional operation). Read Appendix 4 for a more complete discussion.

### Longer Wavelength WDRLs

The basic principles of WDRLs are independent of the wavelength or materials systems used in the laser. However, the etching processes are different for different materials systems.

In particular, materials containing In are more difficult to dry-etch than Ga containing materials, because the In etch products are less volatile. Good dry-etching is essential to WDRLs. Because longer wavelength lasers (1, 1.3, 1.5  $\mu\text{m}$ ) contain In (especially 1.3 and 1.5  $\mu\text{m}$  devices). We developed new etching technology in the National Nanofabrication Facility (NNF) for these materials. The results are described in E. Lemoine's thesis (publication 18). The central result is the necessity to etch In compounds at much higher temperature (200°C) in order to get smooth, vertical surfaces. Lemoine built a special, high temperature stage for the NNF CAIBE system. C. Ji has refined the process, gaining control over etch depth at the high rates involved, and produced WDRL devices in 1.3  $\mu\text{m}$  material. An SEM photo is shown in Fig. 1.

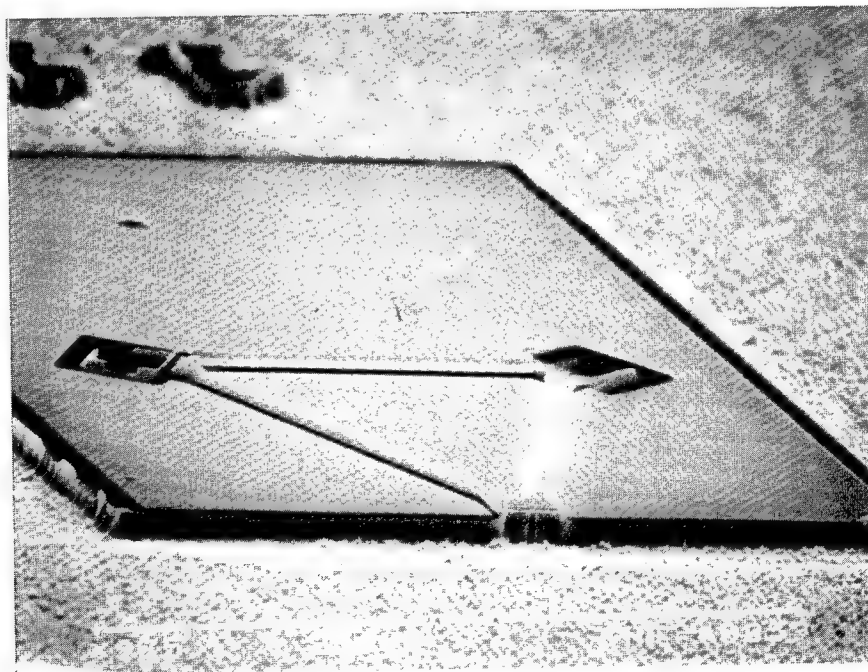


Fig. 1. SEM photo of a 1.3  $\mu\text{m}$  WDRL structure.

The devices have yet to be tested. The spectrum of a 1.07  $\mu\text{m}$  WDRL fabricated in pseudomorphic GaInAs on GaAs using the standard etch process is shown in Fig. 2.

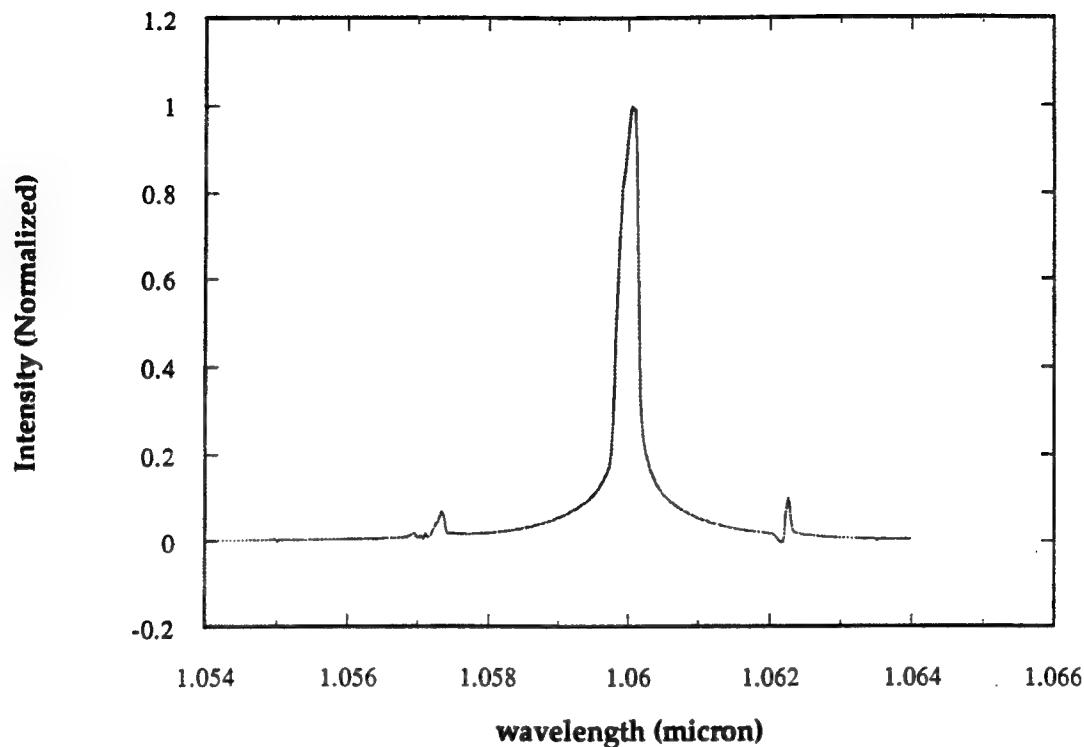


Fig. 2 Spectrum of GaInAs Pseudomorphic WDRL.

MOCVD technology for growing  $1.3\ \mu$  laser material was developed at Cornell as part of this contract. This material has long been produced elsewhere, but at Cornell we have not previously developed an in-house capability. We now have material which is comparable to that from Ortel, who supplied us with several wafers under a collaborative program. Test structures on our material gave thresholds about 5% less than the same structures on Ortel material.

#### Record Performance WDRLs

The WDRLs fabricated under this contract have set world records for the performance of monolithic diode ring lasers including

- cw, room temperature, unpackaged operation
- lowest threshold current (12 ma, single-mode operation)
- highest output power (20 mW unpackaged, single WDRL cf Appendix 3, 85 mW unpackaged WDRL with monolithic  $600\ \mu$  long amplifier cf Appendix 5)
- highest slope efficiency (.28 W/A dual beams cf Appendix 3, .23 W/A single beam cf Appendix 4)
- lowest (only) measured noise (see discussion below)
- shortest length ring laser ( $125\ \mu$ ) operated

In addition these devices showed predictable, reproducible operation which agrees with theory in terms of threshold current variation vs structure angle (Fig. 2, Appendix 2 and Figs. 8 and 9, Appendix 3), far-field pattern,<sup>20</sup> output power vs structure angle (Figs. 11 and 12, Appendix 3), and longitudinal mode spacing (Fig. 15, Appendix 3). They demonstrated side-mode-suppression ratios (SMSR) exceeding 25 dB (publication 7), and a clear relationship between degree of directionality, and SMSR (Fig. 5, Appendix 4).

## Noise Properties

In this work we had much greater difficulty than originally anticipated in making noise measurements on our devices. These difficulties stemmed mainly from two causes: a) getting access to a state-of-the-art measuring apparatus operating in the 800 nm region of our devices, and b) the unpackaged nature of our devices. After pursuing unsuccessfully the possibility of doing our measurements at Rome Labs and four west-coast companies, we finally solved the first problem very late in the contract by procuring our own HP noise measuring system. The unpackaged devices created difficulties for cw operation at high power without degradations, and in efficient coupling of WDRL output light with 1 cm working distance into the single mode fiber required by the measuring system.

Initial relative intensity noise (RIN) measurements have been completed using our HP lightwave analyzer system. The system has a fiber input, and so it was necessary to assemble a customized experimental set up which would allow the laser emission to be coupled into a fiber. A beam splitter and CCD are used to image the near field and aid in the alignment of the laser emission to the single mode fiber.

The coupling efficiency of a commercial Fabry Perot (FP) laser into the analyzer system is about 43%. However, due to the wafer testing of the current devices, the interference patterns that result from this mode of testing and the unusual farfield patterns from the ring lasers, coupling from devices on the wafer is expected to be smaller. The efficiency was measured to be about 23% for an FP laser and 18% for a ring laser. Most of the reduction in the coupling is caused by the need to change to a longer working distance, lower numerical aperture objective lens. This objective lens is necessary due to the constraints on access to the devices imposed by the wafer testing. By using a long working distance, high numerical aperture lens the coupling will increase. Also, in subsequent fabrication runs this access problem will be addressed, and the coupling will be further improved.

Using this set up and the HP equipment, the laser spectra and RIN data were acquired. Heating of the laser devices has been identified as a problem. To help alleviate this problem the device chips were soldered, p-side up, onto a passive heat sink. This action seems to have provided some benefit since the lasers could be operated continuous wave (CW), with threshold currents ranging from 25 to 60 mA. However, despite this effort, the heating problem was not eliminated due

to the large thickness of the chips and the relatively high injection currents that were needed to operate the devices. As a consequence, a number of the lasers degraded in performance, when operated CW, during the RIN testing. This is the reason for some of the variations in the data.

Fortunately, enough preliminary data (about 400 measurements on 6 devices; 4 FP, and 2 WDRLs) was obtained to draw some important conclusions. The results of RIN measurements are shown in Fig. 3.

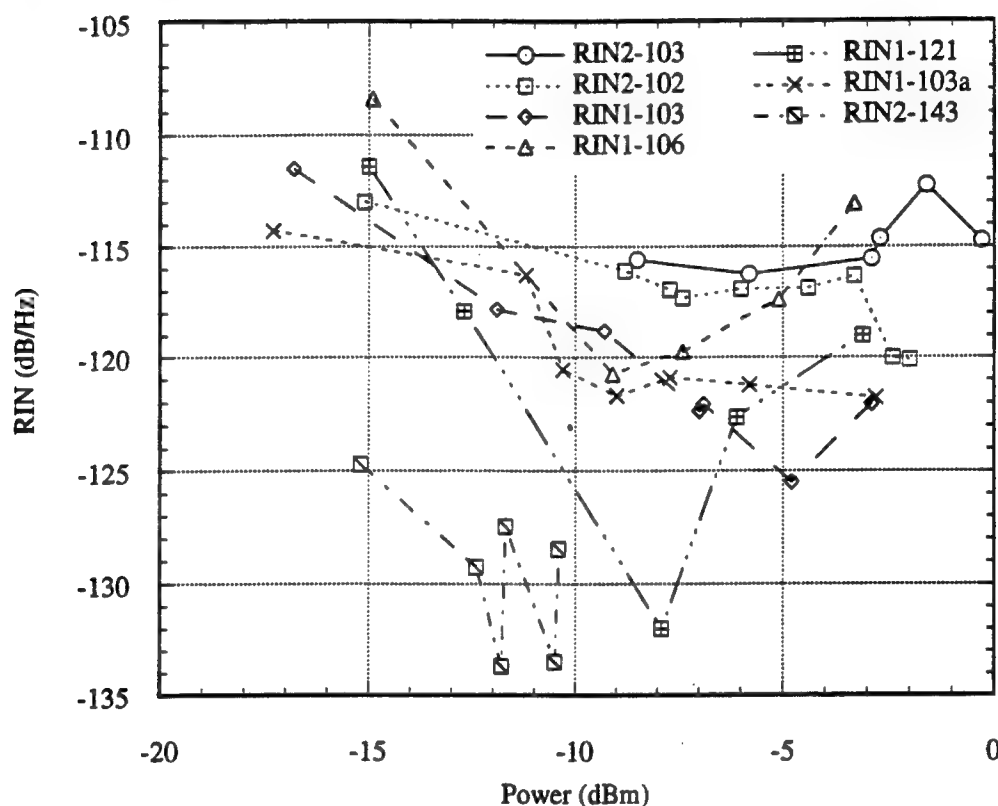


Fig. 3: Measured RIN vs. coupled power level.

As the device drive current was increased, it operated further above threshold, and power coupled into the fiber increased, which is the horizontal axis. Each data point in Fig. 3 is the average of about 10 individual measurements, taken sequentially before proceeding to the next higher drive level. Devices 1-103, 1-106 are FP lasers of length 300 and 600  $\mu\text{m}$ , respectively, in quadrant 1. Devices 2-103 and 2-102 are FP lasers of length 300 and 200  $\mu\text{m}$  in quadrant 2. 1-103a is a subsequent remeasurement of 1-103, and 1-121 and 2-143 are WDRLs in quadrants 1 and 2 respectively. 121 is a 6°, 600  $\mu$  bidirectional ring and 143 an 8°, 800  $\mu$  ring with optical diode. As expected, RIN initially decreases as devices are driven harder (more coupled power). However as drive increases some devices

heat and degrade irreversibly, causing RIN to increase. The RIN of the WDRLs is 10 to 15 dB lower than FP devices and is limited by irreversible degradation because of unpackaged operation. After the RIN data were accumulated, device spectra were taken. The resulting SMSR is shown in Fig. 4.

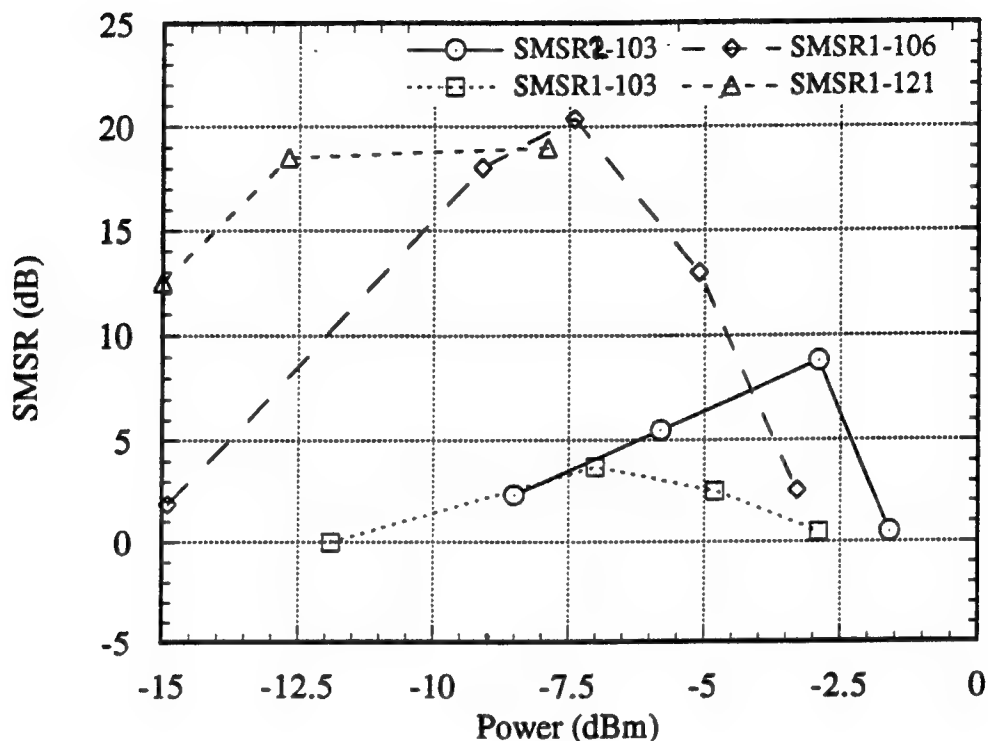


Fig. 4: Side mode suppression ratio vs coupled power level.

Note that 1-106 is a very good FP, and 1-121 a mediocre, bidirectional ring. The SMSR of 106 actually exceeds that of 121. In Fig. 5 we plot RIN vs SMSR for 3 FP and 1 WDRL.



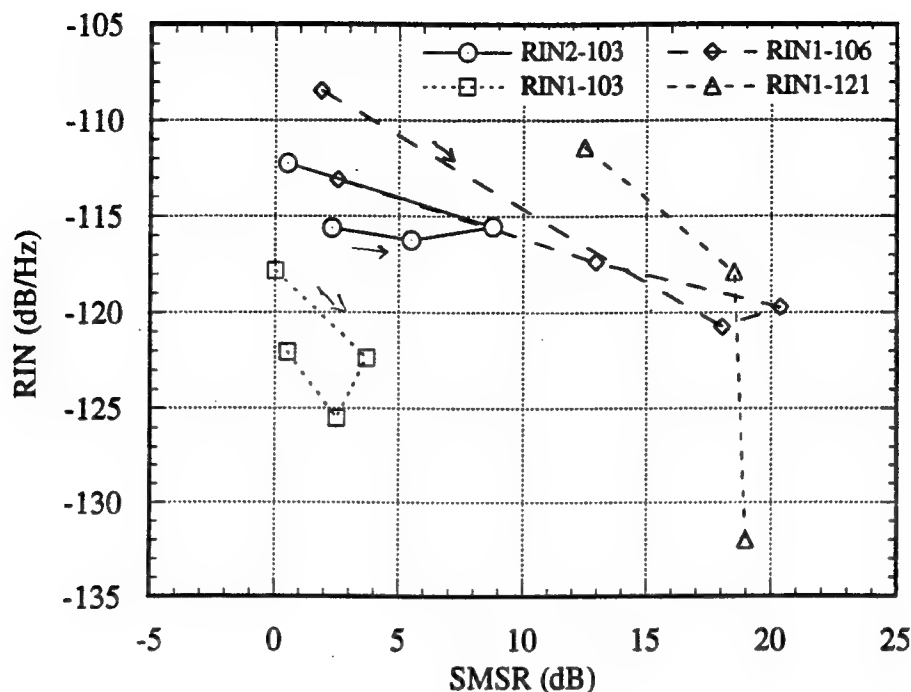


Fig. 5: RIN vs SMSR for Fabry Perot and WDRLs.

Note that the RIN of WDRL 1-121 is decreasing rapidly with drive current, even though its SMSR is not changing much with current. Also note from Fig. 3 that RIN for WDRL 2-143 (with optical diode) is about 15 dB lower than WDRL 1-121 at equivalent output power. We can thus make some extrapolations on the RIN to be expected from properly packaged WDRLs with SMSRs comparable to those measured on better devices. For 2-143 projected operation at coupled power level of -8 dBm, we would guess RIN should be 15 dB lower than 1-121 at that level, or expect a RIN of -147 dBm. Extrapolating the rate of decrease of the RIN for 1-121 to a SMSR of 25 dB measured on other devices, we would expect a RIN between -152 and -216 dBm (the latter clearly impossible) for this bidirectional ring.

The important conclusions are the following:

- RIN of WDRLs is 15-20 dB lower than FP lasers of the same SMSR.
- RIN of optical diode (unidirectional) WDRL is 15 dB lower than for bidirectional WDRL.
- RIN of WDRLs decreases more rapidly with drive current than RIN of FP lasers.
- Trends in RIN decrease with drive current and SMSR are consistent with expectations for both WDRL and FP lasers.
- Trends in RIN decrease of WDRLs with drive current and SMSR lead to projected RINs in the -150 to -170 dBm range for unidirectional, packaged devices at 0 dBm or greater coupled power.

As an aside to the RIN measurement, we measured the noise power spectrum of some FP devices on the chip. An example is shown in Fig. 6.

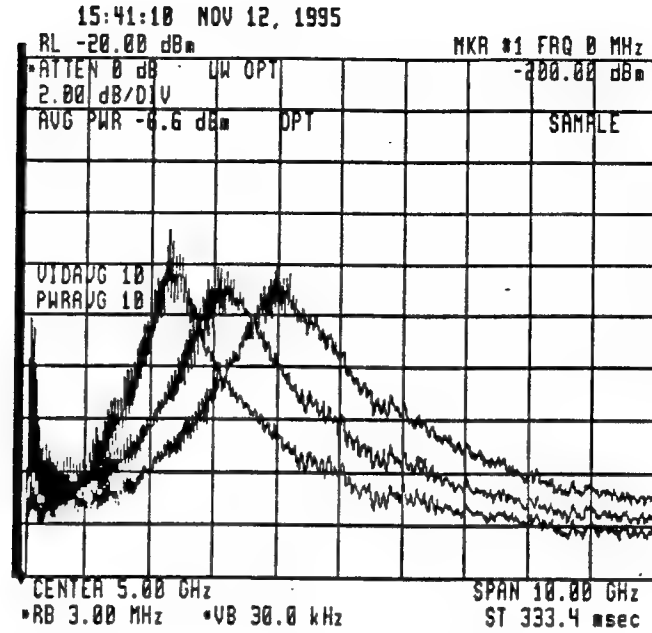


Fig. 6: Noise power spectrum of FP laser 2c-103.  
Left to right  $I_{cw}$  = 33, 37, 44 mA.

As expected, the relaxation oscillation is clearly visible in the 2-4 GHz region. An unusual and unexpected observation during the RIN measurements was the relative temperature dependence of WDRL vs FP emission wavelength. As the devices heated with increased current injection above threshold, the FP spectrum shifted as expected to longer wavelength, while the WDRL spectrum shifted very little. This is an unexpected and potentially very exciting result which we intend to investigate further. The initial result is shown in Fig. 7.

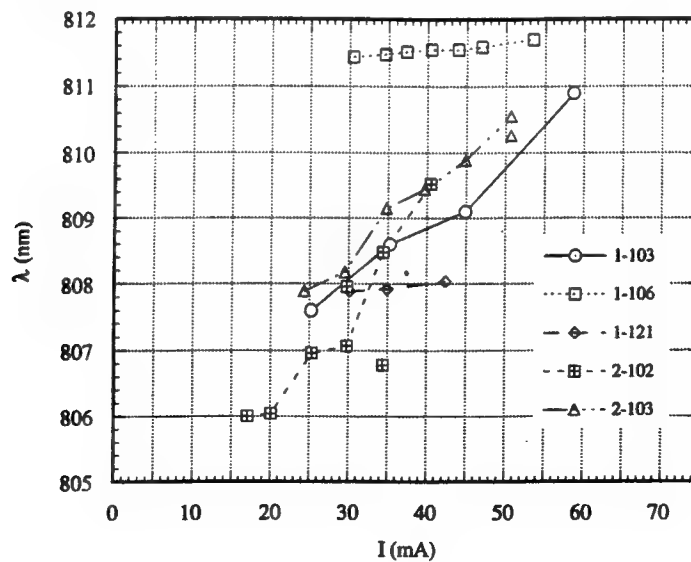


Fig. 7: Current (temperature) dependence of lasing wavelength.

## WDRL Arrays and Integration

Arrays of WDRL devices were produced and tested. Each array contained 12 WDRLs spaced on 250  $\mu\text{m}$  centers to be consistent with fiber ribbon spacing. Some arrays contained coupled waveguides which were oriented for cleaving for passive alignment to fiber ribbons. These arrays gave reasonable performance and uniformity, especially considering there were some process difficulties and they were the first devices produced by a new student. The arrays included solder bump mounting pads for packaging studies. A photo of an array is shown in Fig. 8 and PI curves in Fig. 9. This work showed that there are no particular difficulties in producing arrays of WDRLs and in coupling them to waveguides. Our lowest cw threshold WDRL of 12 ma was measured on this chip (approaching the 10 ma projected minimum limit for this material) as was the operation of our shortest ring (125  $\mu$  length). However the leads connecting solder pads to devices were too thin for extensive testing, as these leads could not carry the current to drive the large lasers. This deficiency has been corrected in a subsequent mask set.

Some of the waveguides were also operated reverse biased as detectors, and we demonstrated the monolithic integration and operation of WDRLs and detectors.

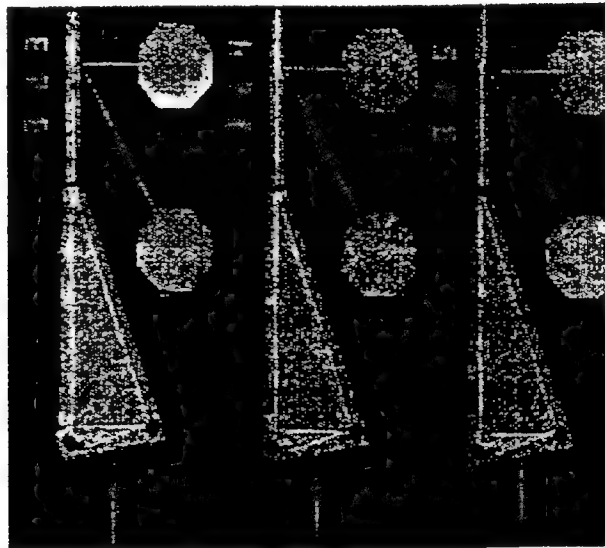


Fig. 8: SEM photo of part of a WDRL array.

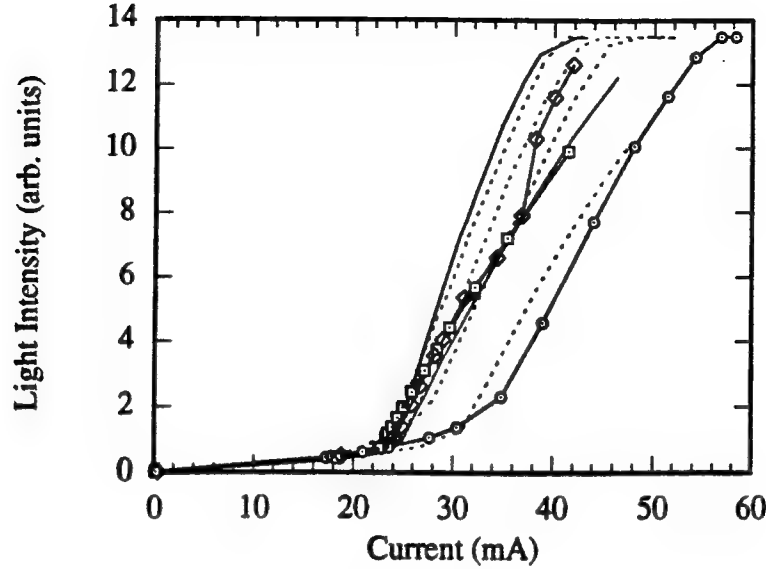


Fig. 9: PI curves of a WDRL array.

### 3. Summary and Outlook

In this program we made major strides in understanding the physics of operation of WDRLs, in developing quantitative tools for modeling WDRL performance, in improving fabrication technologies for these devices, and in demonstrating the exciting potentials for WDRL applications through the excellent (in some areas, record setting) performance of the devices we fabricated. A brief list of accomplishments follows:

- First 3D dielectric turning mirror modeling tool.
- Unique and unusual WDRL far fields predicted and observed.
- First scattering matrix WDRL eigenmode modeling tool.
- 2D boundary element model of WDRL developed.
- WDRL optimized for low threshold current (related program).
- Self aligned, repeatable fabrication process developed.
- Record high quality etched turning mirrors ( $R > 88\%$ ).
- First development of nonreciprocal reflector concept for unidirectional ring lasers.
- First waveguide implementation of nonreciprocal reflector concept.
- Unidirectional (30:1), high SMSR ( $>25$  db) lasers produced.
- Record low threshold (12 mA) single mode ring lasers.
- Record high ring laser external efficiency (0.28 W/A).
- Record high ring laser single beam efficiency (0.23 W/A).
- Record high ring laser output powers (10-20 mW).
- Record output power from first integrated ring laser/tapered amplifier (85 mW).
- Record small WDRL operated (125  $\mu\text{m}$ ).
- WDRL arrays fabricated and tested.
- Hi temperature CAIBE etch for In compounds developed.
- 1.3 and 1.06  $\mu$  WDRL structures fabricated.

- cw, room temperature unpackaged operation of WDRL.
- First RIN measurements on diode ring laser.
- First RIN vs SMSR measurements on WDRL verify low noise capability.
- Monolithic integration of WDRL and detector demonstrated.
- Developed in-house 1.3  $\mu\text{m}$  materials growth capability and demonstrated 1.3  $\mu\text{m}$  lasers.

All results, which are numerous, support the conjectures in the original proposal for the potential of ring lasers in applications requiring high spectral purity, low noise, small, manufacturable, efficient and even high power sources. We have shown that these devices have a unique combination of properties unmatched by a competitor. Their noise and spectral purity are comparable to DFB lasers, but they have higher power, are smaller, are easier to integrate, possibly operate without isolators, and should be much cheaper to manufacture. They can be made nearly as small as SELs, are probably easier and cheaper to manufacture, probably have lower noise, emit higher power, and are easier to integrate with planar waveguides besides not requiring isolators.

The areas of our work which came short of initial expectations included full exploration of the noise properties of WDRLs, which will require advanced packaging of devices not contemplated in this work, and full development of finite element modeling for predictive unidirectional device design. Work in both areas is ongoing and will be carried through in a new Air Force program to develop laser modules from these devices.

The future outlook is extremely bright for the development of high power, low noise sources. In addition, new applications may arise as we explore more fully the temperature dependence and dynamic properties of WDRLs. A totally different set of applications, with huge potential impact exploits the small size, potential low threshold, efficiency, manufacturability, and integrability of these devices. Under SRC and some separate Rome Lab funding we are exploring the possibility of developing a materials system lattice-matched to Si so that small WDRLs can replace output pads in Si chips. Such a development would also impact low noise/high power applications, as it would greatly simplify packaging and facilitate passive alignment to fibers, while providing better heat sinking and lower cost.

#### 4. Publications List

- 1\*. "Reflection and Transmission of a Dielectric Waveguide Mirror", T. Shiraishi, S.T. Lau, A. Behfar-Rad, J.M. Ballantyne; LEOS '91 Conference Digest 21 (1991).
- 2\*. "Analysis of Guided Wave Diode Ring Laser Operation", S.T. Lau, T. Shiraishi, J.M. Ballantyne; LEOS '91 Conference Digest 54 (1991).
- 3\*. "Reflection and Transmission of a Dielectric Waveguide Mirror", S.T. Lau, T. Shiraishi, P. McIsaac, A. Behfar-Rad and J.M. Ballantyne; *IEEE J. Lightwave Technology*, 10, 634 (1992).
- 4\*. "Guided Wave Diode Ring Lasers for Monolithic Optoelectronics", J.M. Ballantyne, Program 1992 IEEE C31 Technology and Applications Conference, p. 14, June 1992.
5. "Self-aligned Single-lateral-mode Waveguide Diode Ring Lasers", James J. Liang and Joseph M. Ballantyne. *IEEE LEOS '93 Conference Proceedings*, p. 621, Nov. (1993).
6. "Scattering Matrix Analysis of a Triangular Ring Laser", S.T. Lau, T. Shiraishi, and J.M. Ballantyne, *IEEE Journal on Lightwave Technology* 12, 202 (1994).
7. "Monolithic Ring Lasers for Low-noise Signal Distribution", James J. Liang and Joseph M. Ballantyne. *Proceedings SPIE OE/LASE '94 Conference*, Jan. 1994, Los Angeles, CA, paper #2155-16 (to be published '94).
8. "2-D Analysis of a Dielectric Waveguide Mirror with Application to a Diode Ring Laser Operation", S.T. Lau and J.M. Ballantyne. *Proceedings IEEE Dual Use Technologies & Applications Conference*, 23 May 1994, Utica, NY, Vol. II, p. 213-216.
9. "2-D Analysis of a Dielectric Waveguide Mirror", S.T. Lau and J.M. Ballantyne. *Proc. IEEE LEOS '94*, 55, 1994.
10. "Unique Aspects of Waveguide Diode Ring Lasers", J.J. Liang, S.T. Lau, and J.M. Ballantyne, *Proc. IEEE LEOS '94*, 393, 1994.
11. "Analysis of Reflection and Transmission of a Multi-Mode Dielectric Waveguide Mirror", T. Shiraishi, S.T. Lau, and J.M. Ballantyne, submitted to *IEEE Journal on Lightwave Technology*.
12. "Self Aligned Dry Etching Process for Waveguide Diode Ring Lasers", James J. Liang and Joseph M. Ballantyne, *J. Vac. Sci & Technol. B* 12, 2929, 1994.
13. "Self-aligned V-shaped Lasers and Triangular Ring Lasers", J.J. Liang, M.H. Leary, S.T. Lau, and J.M. Ballantyne. Submitted to *IEEE J. Lightwave Technol.*

---

\* This work was published prior to the start of this contract.

14. "Monolithic Integration of Tapered Amplifiers with Ring Lasers", J.J. Liang and J.M. Ballantyne. Submitted to *Applied Phys. Lett.*
15. "Unidirectional Operation of Waveguide Diode Ring Lasers", J.J. Liang, S.T. Lau, M.H. Leary, and J.M. Ballantyne. Submitted to *Applied Phys. Lett.*
16. "Self-aligned Single-lateral-mode Waveguide Diode Ring Lasers", J.J. Liang, S.T. Lau, M.H. Leary, and J.M. Ballantyne. Submitted to *IEEE J. Lightwave Technology*.
17. "Chlorine Reactive Ion Beam Etching Studies of Indium-containing III-V Materials", Eugene E. Lemoine, M.S. Thesis, Cornell University, Aug. 1994.
18. "Monolithic Waveguide Diode Ring Lasers for Low Threshold and Low Noise Operation", James J. Liang, Ph.D. Thesis, Cornell University, Jan. 1995.
19. "Modeling of a Dielectric Waveguide Mirror with Application to Diode Ring Lasers", Stanley T. Lau, Ph.D. Thesis, Cornell University, June 1995.
20. "Manual for Programs for the 2-D Mode Analysis of a Dielectric Waveguide Mirror and The Scattering Matrix Analysis of the Triangular Ring Laser", Stanley T. Lau, Technical Report, Cornell University, June 1995.

## **5. List of Personnel**

The following personnel contributed to work under this contract.

Dr. Joseph M. Ballantyne, Professor of Electrical Engineering, Cornell University

Dr. Yossi Salzman, Visiting Assoc. Professor of Electrical Engineering, Cornell  
Associate Professor of Electrical Engineering, Technion, Israel

Dr. Dan Fekete, Visiting Scientist, Cornell  
Associate Professor of Physics, Technion, Israel

Dr. Simon Gdzelishvili, Visiting Scientist, Electrical Engineering, Cornell  
Senior Lecturer, Technical University, Tbilisi, Republic Georgia

Dr. A. Schremer, Research Associate in Electrical Engineering, Cornell

\*Dr. S. T. Lau, Postdoctoral Associate in Electrical Engineering and  
Graduate Research Assistant in Electrical Engineering, Cornell

\*Dr. J. L. Liang, Graduate Research Assistant in Physics, Cornell

M. Leary, Graduate Research Assistant in Electrical Engineering, Cornell

Karen Wilson, GTE Fellow and Graduate Research Assistant in Electrical  
Engineering, Cornell

J. Lee, Graduate Research Assistant in Applied Physics, Cornell

\*E. Lemoine, Graduate Research Assistant in Materials Science, Cornell

Chen Ji, Kodak Fellow and Graduate Research Assistant in Physics, Cornell

M. Booth, NSF Fellow and Graduate Research Assistant in Physics, Cornell

### **Graduate Degrees**

\*S. Lau completed the Ph.D. degree in Electrical Engineering; J. L. Liang, the Ph.D. degree in Physics; and E. Lemoine, the M.S. degree in Materials Science under this program.



## **Appendix 1: Excerpt from the Original Proposal (1992)**

### **Technical Background**

Semiconductor ring lasers in a variety of forms have been studied since the early days of semiconductor laser research.<sup>1-6</sup> Recently, facet formation through the use of dry-etching techniques has allowed crystal-orientation-independent facets to be fabricated which have reflectivities that are similar to cleaved facets.<sup>6,7</sup> Taking advantage of the flexibility of such techniques, we first demonstrated monolithic broad-area ring lasers and subsequently built the first diode ring lasers in low-order dielectric waveguide. These devices showed the first traveling wave operation in monolithic diode lasers.<sup>9</sup>

#### Properties of Diode Ring Lasers

Recently, a process was reported which made use of dry-etching for both the facet and the ridge to fabricate single-mode ridge lasers in the GaAs/AlGaAs material system.<sup>10</sup> Using this process, triangular-shaped ring ridge lasers have been fabricated using thin-cladding, graded-index, separate-confinement-heterostructure, single-quantum-well material. A scanning electron microscope photograph of a triangular ring ridge laser is shown in reference 9. The device has two total-internal-reflection facets and one output facet that allows partial transmission. The spectrum of a triangular ring ridge laser is also shown in Ref. 9. At threshold, the laser demonstrates multi-longitudinal-mode behavior. Above threshold, however, the device becomes single longitudinal-mode, characteristic of a traveling wave laser. Etched facet Fabry-Perot ridge lasers of comparable dimensions demonstrated multi-longitudinal-mode behavior above threshold. The horizontal far-fields for triangular ring lasers with 3.5 and 2.5  $\mu\text{m}$  wide ridges<sup>9)</sup> show that both bidirectional and unidirectional operation are possible. The unidirectional behavior is achieved in a lossy waveguide that allows only one lateral mode and which apparently has greater loss in one direction of propagation in the ring laser than the other. This non-reciprocal behavior is geometrically controlled and probably arises from fabrication asymmetries such as a difference in the incidence angles of the two legs of the triangular ring ridge laser to the output facet. Such behavior contrasts with conventional non-reciprocal operation of devices that rely on magnetic fields. Bidirectional triangular ring ridge lasers were fabricated with different incidence angles,  $\Theta_i$ , to the output facet. The angular separation between the peaks of the two lobes in the horizontal far-field is equivalent to twice the emergence angle,  $\Theta_0$ .  $\Theta_0$  values, obtained from far-field measurements of triangular ring ridge lasers with different  $\Theta_i$  values,<sup>9)</sup> show that for  $\Theta_i$  values up to about 3 degrees below the critical angle,  $\Theta_0$  follows the plane-wave approximation and Snell's law very closely. However, near and above the critical angle, the plane-wave approximation breaks down, and in contrast to broad-area devices, output is obtained even above the critical angle.

## Uniqueness of Diode Ring Lasers

These triangular ring lasers<sup>8</sup> were the first demonstration of a technique for fabricating semiconductor laser resonators of variable  $Q$  using geometry alone as the variable. This is very important for monolithic integration, since cavity  $Q$  has a major impact on threshold current, cavity size, modulation rate, and output power. The ability to fabricate variable  $Q$  resonators in a planar and manufacturable fashion opens new vistas for monolithic integration of lasers which can be optimized for appropriate combinations of the foregoing parameters.

The unidirectional operation of the ring laser is also an extremely significant point: if the output is reflected back into such a unidirectional ring laser it couples into a non-oscillating mode of the cavity, and hence should have substantial impact on reducing reflection induced intensity noise. It may also obviate the need for optical isolators in order to prevent reflections from entering the transmitting laser and hence greatly simplify monolithic optical transmitters.

The triangular resonator geometry utilized in our work has a further singular advantage over all of the earlier semiconductor ring laser work,<sup>2-6</sup> since it provides a controllable amount of output coupling. The early work was generally done in rectangular cavities where all facets were totally reflecting and hence no light was coupled out, except for spurious scattered light. A major problem of those investigators was to try and get light out of their cavity to demonstrate that the lasers were in fact operating. Various schemes were utilized including coupling the ring to other waveguides in order to extract power. Such complicated output coupling schemes are obviated by the triangular ring geometry that we introduced.

## Modeling of Diode Ring Lasers

Since our experimental demonstration of the promise of diode ring lasers, we have conducted theoretical modeling investigations of the cavity to understand features such as output coupling beyond the critical angle, farfield patterns, and unidirectionality. We have done two types of modeling: a) simulation of the beam propagation through a triangular turning mirror including effects of output coupling,<sup>12</sup> and b) eigenmode analysis of the entire laser resonator consisting of three triangular turning mirrors.<sup>13</sup> Results of the first investigation (which is a 2-dimensional analysis and neglects mode shape perpendicular to the waveguide plane) predicted forward, reverse and output coupling vs. structure angle and facet tilt and offset, and far-field angles. The computed emergence angle agrees in general with the experimental results.<sup>12)</sup> The computed forward interwaveguide coupling as a function of mirror asymmetry shows that asymmetric forward coupling is probably not the cause of the observed unidirectional operation, even though such a model has been proposed in the literature.<sup>11</sup> Results of the eigenmode analysis indicate that a small asymmetry in intrawaveguide back reflection at a triangular turning mirror could account for a large asymmetry in power circulation in the two directions in the resonator. An asymmetry of back reflection of 1% at a waveguide junction could explain a ratio of nearly 100 in intensities in the two counter propagating modes. However, using the reflecting corner analysis we compute significant differences in

reflectivity only for very small incident angles, in contrast with the experimental observation. However, validity of our Fourier transform method for analyzing the corner reflectors also breaks down at small angles of incidence, and the approach in general neglects details of the sharp geometries at the vertices which are undoubtedly significant in effecting small amounts of forward and backward coupling. We are unable therefore at present to give an unambiguous explanation from our modeling of the reasons for unidirectional operation in these devices, although we understand which aspects of our modeling need to be improved to give a more realistic picture of the actual situation.

### Noise Considerations in Guided Wave Diode Ring Lasers

**Relative Intensity Noise (RIN) can be substantially reduced by eliminating mode partition noise.** Mode partition noise is the major noise component in most Fabry-Perot (FP) diode lasers. It is especially severe during turn on transients. It is directly related to the degree to which the resonator is single mode and hence suppresses its side modes. It has been shown by Liu<sup>14</sup> that mode partition noise becomes negligible if the side mode suppression ratio (SMSR) is greater than -17db at bias or -35db under modulation. Ring lasers have historically been noted for oscillating in pure single modes. Experimental data for our first guided wave ring lasers provided a direct experimental comparison between the mode spectra of the ring lasers and that of straight lasers of comparable length fabricated using identical technology on the same wafer. All of the ring lasers showed a very strong tendency towards single longitudinal mode operation with substantial suppression of side modes. This was in great contrast to the similar, FP cavity devices all of which oscillated in 6 to 10 longitudinal modes. Although we produced hundreds of ring lasers, we only measured spectra on 7 or 8. The best of these gave a SMSR of 40 to 1. The -17db suppression corresponds to 50 to 1. In our first attempt we have apparently inadvertently produced at least one laser with nearly sufficient side mode suppression ratio at bias to eliminate mode partition noise as a consideration. The spectra we took on our ring lasers were all from ring lasers operating bidirectionally. Because of spatial hole burning in the gain of a bidirectional ring laser, we would expect the mode spectra to be less pure than in a unidirectional pure traveling wave ring laser. We produced such ring lasers but were not able to measure their mode spectra.

There is apparently no model for predicting a priori the SMSR in diode laser resonators. Hence we cannot compute the value for the best possible SMSR in a unidirectional ring laser, but we are confident, based on our initial experimental observations, that it will be better than any FP diode laser by a substantial margin. A recent ridge guide FP diode laser (H. Jaekel et al.<sup>15</sup>) gave RIN below -150db, and the measure was limited by the instrument limit. This is the same waveguide and material that we use in the ring laser, hence we are confident that we can easily surpass -150db.

**High differential gain is needed for narrow linewidth laser operation.** The linewidth  $\Delta f$  of a diode laser is roughly proportional to  $(I - I_{th})^{-1}$ . Because a unidirectional diode ring laser contains a pure traveling wave in one direction, as opposed to the normal case of waves traveling in both directions which pertains to

a FP laser or a bidirectional ring, the differential gain for a unidirectional ring will be twice that of a bidirectional laser. From this we have computed the linewidth ratio of a unidirectional laser to a bidirectional laser oscillator. Until one gets to several times threshold for the bidirectional laser, the unidirectional laser has a substantially narrower linewidth than does the bidirectional laser. Just above threshold this linewidth is less than one-tenth that of the bidirectional laser.

Once the mode partition noise is eliminated, then these intrinsic linewidth considerations become important, and the narrower the linewidth the lower the noise of the laser. The unidirectional ring is seen to have substantial advantage over any bidirectional laser in this respect. This is consistent with the fact that the narrowest linewidth lasers are always unidirectional rings, and such a unidirectional ring Nd YAG laser is used by Hewlett-Packard as a standard in their optical measuring instrumentation.

**Large, high Q cavities have lower noise.** The relative magnitude of the fluctuating to the average component of photon density becomes smaller as the total number of photons in the cavity is increased. This argues for as large an optical cavity as possible. The diode lasers showing the lowest RIN are usually long cavity lasers. Liu<sup>14</sup> showed that an external cavity laser with a 6.5 cm cavity had extremely low noise. The Jaeckel<sup>15</sup> laser also has a relatively long cavity, of 750 microns, and is driven at many times threshold. A disadvantage of external cavities is their large size, occasioned by the mechanical components necessary, and by their sensitivity to mechanical disturbances. They are also not cheap to fabricate. The monolithic ring can be made with large total photon path length, while occupying a relatively smaller substrate area than a straight laser, and in addition provides a very high Q cavity without the necessity of mirror coatings. The total number of photons in the mode is also increased by raising the cavity Q. Both the long cavity and a high Q aid in high spectral selectivity with narrow linewidth. In both these aspects the ring lasers will excel FP or DFB lasers.

Another way to get high photon flux is to drive the laser hard. This can be done with both ring and FP lasers, but the ring laser will have no special advantage, or disadvantage, in this regard. We will build our ring lasers with pseudomorphic active layers and ridge waveguides which have been demonstrated to produce the highest photon density of any semiconductor laser.

**A high Q cavity reduces the K factor.** The monolithic ring laser is ideal for producing high Q cavities as its loss is controlled by geometry only. In addition, a unidirectional traveling wave ring laser will have no longitudinal non-uniformities due to gain saturation. Hence it is the ideal case for a small K factor.

**For low noise the resonator acceptance angle for spontaneous emission should be very small.** The rib waveguide of our ring lasers is an ideal vehicle for achieving a weak index guide, which when combined with long cavity length and with the selective properties of the turning mirrors will produce an extremely small acceptance angle towards spontaneous emission. The amount of spontaneous emission captured by the resonator should be several orders of magnitude lower than that of today's typical FP diode lasers.

**Conclusion.** All factors affecting linewidth and intensity noise point to the unidirectional ring rib waveguide diode laser as having the lowest possible noise of any monolithic semiconductor laser. Indeed the noise level of these lasers should be identical to that of a quietly pumped solid state laser (such as Nd YAG) with the same cavity volume. We are therefore confident that such lasers can be made to yield RINs on the order of -165db or less. We will need special procedures to measure such low RINs.

## **References**

1. This discussion follows closely the text of reference 9.
2. J. Hayashi and M.B. Panish, J. Appl. Phys. **41**, 150 (1970)
3. D.R. Scifres, R.D. Burnham, and W. Streifer, Appl. Phys. Lett. **28**, 681 (1976)
4. N. Matsumoto and K. Kumabe, Jpn. J. Appl. Phys. **16**, 1395 (1977)
5. A. Liao and S. Wang, Appl. Phys. Lett. **36**, 801 (1980)
6. F. Shimokawa, H. Tanaka, R. Sawada, and S. Hara, Appl. Phys. Lett. **56**, 1617 (1990)
7. A. Behfar-Rad, S.S. Wong, J.M. Ballantyne, B.A. Soltz, and C.M. Harding, Appl. Phys. Lett. **54**, 493 (1989)
8. A. Behfar-Rad and S.S. Wong, IEDM Technical Digest, 319 (1988)
9. A. Behfar-Rad, S.S. Wong, and J.M. Ballantyne, IEDM Technical Digest 6.8.1 (1990)
10. A. Behfar-Rad and S.S. Wong, CLEO Technical Digest, 470 (1990)
11. A. Sennaroglu and C.R. Pollock, J. Lightwave Technol. **9**, 1094 (1991)
12. T. Shiraishi, S.T. Lau, A. Behfar-Rad and J.M. Ballantyne, LEOS paper OE 2.2, San Jose, Nov. 1991.
13. S.T. Lau, T. Shiraishi and J.M. Ballantyne, LEOS paper SDL 10.6, San Jose, Nov. 1991.
14. P.L. Liu, Chapter 10 in Coherence, Amplification and Quantum Effects in Semiconductor Lasers, Y. Yamamoto, ed., John Wiley & Sons (1991).
15. H. Jaeckel et al., J. Quantum Electron. **27**, 1560 (1991)
16. J.D. Ralston, S. O'Brien, G.W. Wicks and L. F. Eastman, Appl. Phys. Lett. **52**, 1511 (1988).

## **Self-Aligned Single-Lateral-Mode Waveguide Diode Ring Lasers**

**James J. Liang<sup>\*</sup>, Stanley T. Lau, Michael H. Leary, and Joseph M. Ballantyne**

**School of Electrical Engineering,  
Cornell University,  
Ithaca, NY 14853**

**<sup>\*</sup> Dept. of Physics, Cornell University, Ithaca, NY 14853**

### **ABSTRACT**

A self-aligned process is used, for the first time, to fabricate triangular semiconductor ridge ring lasers. The dependence of the threshold current for the ring lasers on the structure angle is demonstrated, consistent with reflectivity calculations. The ring lasers show stronger tendency toward single-longitudinal-mode operation than the Fabry-Perot lasers fabricated on the same wafer. The introduction of an external mirror reflector (EMR) in the ring laser structure results in highly asymmetric output and further enhances the side-mode-suppression-ratio (SMSR).

## Self-Aligned Single-Lateral-Mode Waveguide Diode Ring Lasers

Advancement in modern monolithic integration and processing technology has allowed semiconductor lasers of more complicated geometry to be fabricated. Ring diode lasers are gaining popularity; in fact, a number of different types of ring cavities have been reported including circular [1]-[3], oval [4], square [5], and triangular [6], [7]. Of all the ring geometries reported, the triangular cavity is particularly promising, because it possesses the ability of varying the cavity-Q simply by adjusting the cavity design. In addition, the triangular cavity provides ring laser operation on a much reduced size scale compared to the circular and oval lasers, and yet without the output coupling problems of the square laser. In this letter, we present a combination of significant new experimental results on the operating characteristics of the triangular ring lasers we fabricated, which demonstrate the unique aspects of these lasers.

The majority of the ring lasers reported to date, have been formed by etching the waveguide through the entire active region [1]-[5], which results in multi-lateral-mode operation. In order to make single-lateral-mode ring lasers, the waveguide and the facets have to be etched separately, with the facets deep-etched, but the waveguide shallow-etched. The first single-lateral-mode waveguide diode ring lasers were demonstrated by Behfar-Rad et. al. [6]; those ring lasers were triangular-shaped, with the ridge and the facet positions defined by two separate lithography steps. In this approach, the facets, due to inevitable alignment errors, could be displaced from their ideal positions, thus causing additional losses. In this work, we have applied, for the first time, a self-aligned etching process in which both the ridge and the facets are defined by the same lithography step, to fabricate diode ring lasers.

Our self-aligned etching process permits the use of a smooth dielectric masking layer and allows the deep facet etch to be completed in one single step.

Shown in Fig. 1 (a) is the fabricated triangular ring laser, which consists of three straight ridge sections meeting at two totally reflecting facets at the bottom and one output facet at the top. And shown in Fig. 1(b) is a schematic drawing of the triangular ring cavity, with the structure angle  $\theta$  defined. The epitaxial layer is an AlGaAs/GaAs single quantum well graded index separate confinement heterostructure (GRINSCH-SQW) grown by Molecular Beam Epitaxy (MBE), with the quantum well being  $\text{Al}_{0.08}\text{Ga}_{0.92}\text{As}$ . Both the ridge and the facets for the ring lasers are dry-etched by chemically assisted ion beam etching (CAIBE) using plasma enhanced chemical vapor deposition (PECVD)  $\text{SiO}_2$  as the etch-mask, the ridge is shallow-etched stopping slightly above the active region allowing single-lateral-mode operation. The self-aligned etching process is described in detail elsewhere [8].

All the lasers were tested under pulsed condition. TE polarization is observed for the ring lasers. In an experiment to investigate the threshold dependence on the structure angle, ring lasers with a fixed cavity length of  $400\text{ }\mu\text{m}$  and ridge width of  $3.5\text{ }\mu\text{m}$ , but with varying structure angles were fabricated. Shown in Fig. 2 is the measured threshold current density (the right axis) for the ring lasers as a function of the structure angle, as well as the calculated  $\ln(1/R)$  term (the left axis) for TE polarization using a 2-D analysis [9], where  $R$  is the effective reflectivity combining all three mirrors. As we can see from Fig. 2, good agreement is found between the experimental data and the theoretical predictions for TE modes. Therefore, we have successfully demonstrated the threshold current dependence on the structure angle for the ring lasers, consistent with reflectivity calculations. This in turn illustrates



the potential of these lasers to have adjustable cavity-Q with the design of structure parameters.

We have built Fabry-Perot lasers as well as ring lasers on the same wafer, the ring lasers showed a much stronger tendency toward single-longitudinal-mode operation than the Fabry-Perot lasers. Shown in Fig. 3 is the comparison between the spectrum of a Fabry-Perot laser with a cavity length of  $650\text{ }\mu\text{m}$  and that of a ring laser with a cavity length of  $800\text{ }\mu\text{m}$  at comparable injection currents; the side-mode-suppression-ratio (SMSR) of the ring laser is 17 dB, while that of the Fabry-Perot laser is only 9 dB.

For some of the ring lasers, we fabricated an external mirror reflector (EMR) in the way of one of the output beams, so that some light can be reflected back into the cavity, thus introducing an asymmetric backward coupling [10] for the two counter-propagating modes. Fig. 4 shows the lateral far field patterns for both a standard ring laser and a ring laser with EMR; the standard ring laser exhibits bi-directional output with two equal intensities, while the ring laser with EMR shows highly asymmetric output, with the output power ratio between the two beams being 10 to 1. In the direction without the EMR, the output beam is found to be the dominant one, which we think is a result of the preferential backward coupling provided by the EMR into this circulating direction. In order to make sure that the observed asymmetric far field is not a result of the EMR blocking the output, the detector used to measure the far field is tilted downward at a sufficient angle so that only the unobstructed part of the beam is observed.

Furthermore, the SMSR is enhanced for these highly asymmetric ring lasers with EMR's. Fig. 5 (a) is the SMSR of a ring laser with EMR and a cavity length of

800  $\mu\text{m}$  as a function of the injection current, and the spectrum for this laser at an injection current of 100 mA is shown in Fig. 5 (b). At this current, the laser exhibits a SMSR of 25 dB. Since the lasers were tested under pulsed condition, we expect the continuous-wave SMSR to be even better with the elimination of turn-on and turn-off transients.

In conclusion, a self-aligned process is used, for the first time, to fabricate waveguide diode ring lasers, thus eliminating losses and other complications caused by facet displacement. This self-aligned etching process allows the fabrication of optical cavities with predictable characteristics from modeling. Ring lasers with various structure angles were fabricated, and the experimental and theoretical results for the threshold current dependence on the structure angle agree closely. The ring lasers show stronger tendency toward single-frequency operation than the Fabry-Perot lasers fabricated on the same wafer, with an increase of about 8 dB in the SMSR. With the introduction of EMR in the ring laser structure, highly asymmetric output is obtained, which further enhances the SMSR.

#### ACKNOWLEDGMENT

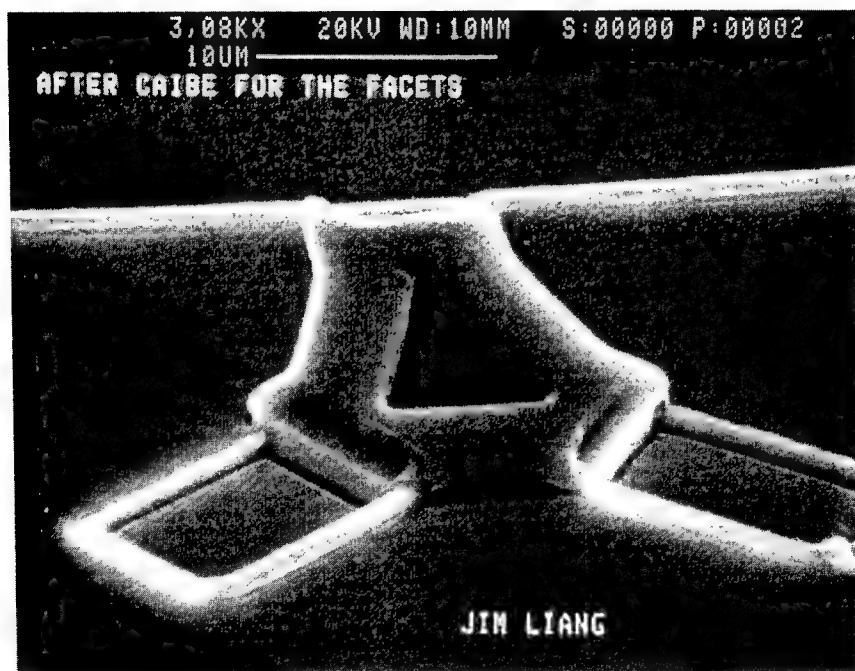
This work was funded by the Air Force and ARPA under Rome Laboratory Contract No. F30602-92-C-0082, and GE (now Martin Marietta). All fabrication was performed at the National Nanofabrication Facility which is supported by the National Science Foundation, Cornell University, and Industrial Affiliates. We would like to thank Dr. A. Behfar-Rad for fruitful discussions and Dr. G. Porkolab for his help in the process development.

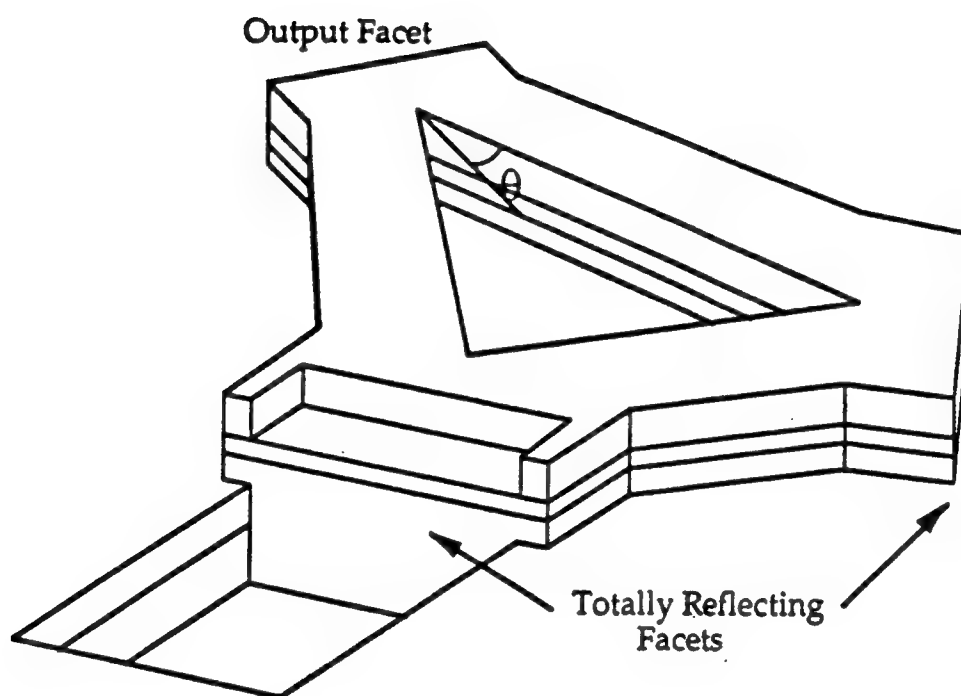
## REFERENCES

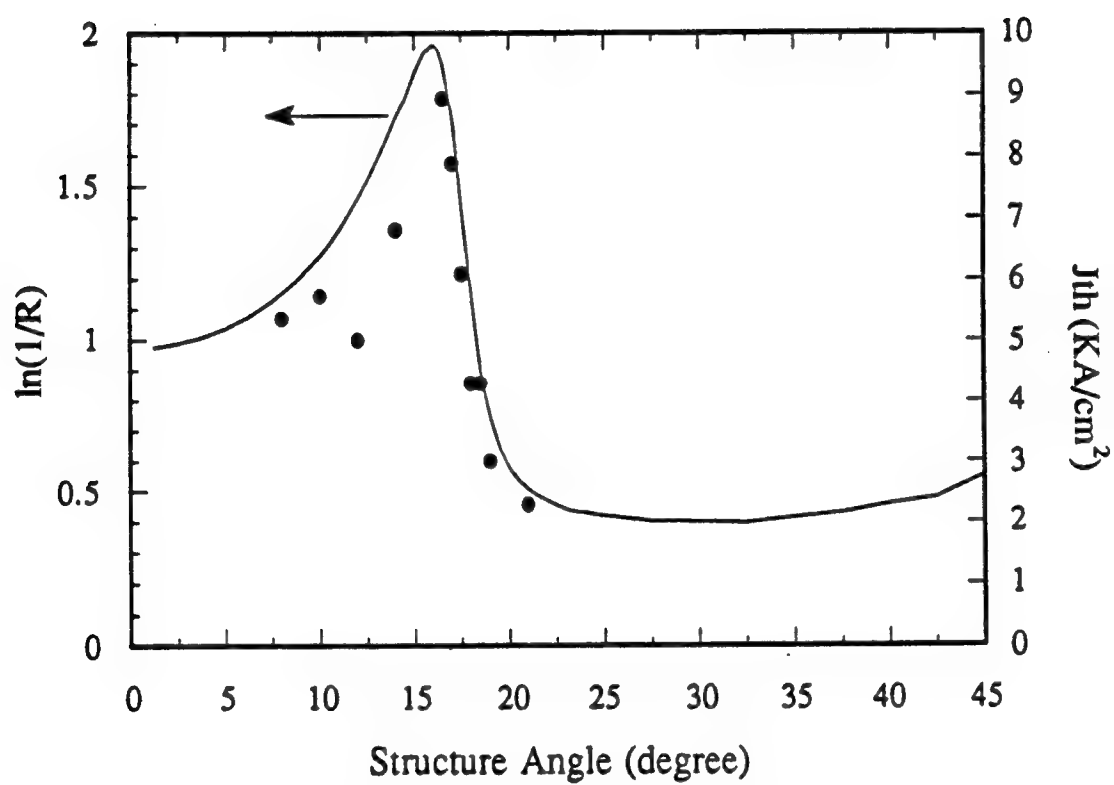
- [1] T. Krauss, P.J.R. Laybourn, and J. Roberts, "CW operation of semiconductor ring lasers," *Electron. Lett.*, vol. 26, pp. 2095, 1990.
- [2] J.P. Hohimer, D.C. Craft, G.R. Hadley, G.A. Vawter, and M.E. Warren, "Single-frequency continuous-wave operation of ring resonator diode ring lasers," *Appl. Phys. Lett.*, vol. 59, pp. 3360, 1991.
- [3] H. Han, M.E. Favaro, D.V. Forbes, and J.J. Coleman, " $\text{In}_x\text{Ga}_{1-x}\text{As}-\text{Al}_y\text{Ga}_{1-y}\text{As}$ -GaAs strained-layer quantum-well heterostructure circular ring lasers," *IEEE Photon. Technol. Lett.*, vol. 4, pp. 817, 1992.
- [4] J.P.Hohimer, G.A.Vawter, and D.C.Craft, "Unidirectional semiconductor ring lasers," in *Technical Digest of CLEO'93*, pp. 266, 1993.
- [5] S. Oku, M. Okayasu, and M. Ikeda, "Low-threshold CW operation of square-shaped semiconductor ring lasers," *IEEE Photon. Technol. Lett.*, vol. 3, pp. 588, 1991.
- [6] A. Behfar-Rad, S.S. Wong, and J.M. Ballantyne, "Traveling-wave operation in a triangular-shaped monolithic semiconductor ring ridge laser," *Proc. IEDM* 6(8), pp. 1, 1990.
- [7] A. Behfar-Rad, J.M. Ballantyne, and S.S. Wong, "AlGaAs/GaAs-based triangular-shaped ring ridge lasers," *Appl. Phys. Lett.*, vol. 60, pp. 1658, 1992.
- [8] J.J. Liang and J.M. Ballantyne, "Self-aligned dry-etching process for waveguide diode ring lasers," accepted by *J. Vac. Sci. Technol. B*.
- [9] S.T. Lau and J.M. Ballantyne, "2-D analysis of a dielectric waveguide mirror," accepted by *IEEE LEOS'94 Conference*.
- [10] S.T. Lau, T. Shiraishi, and J.M. Ballantyne, "Scattering matrix analysis of a triangular ring laser," *J. Lightwave Technol.*, vol. 12, pp. 202, 1994.

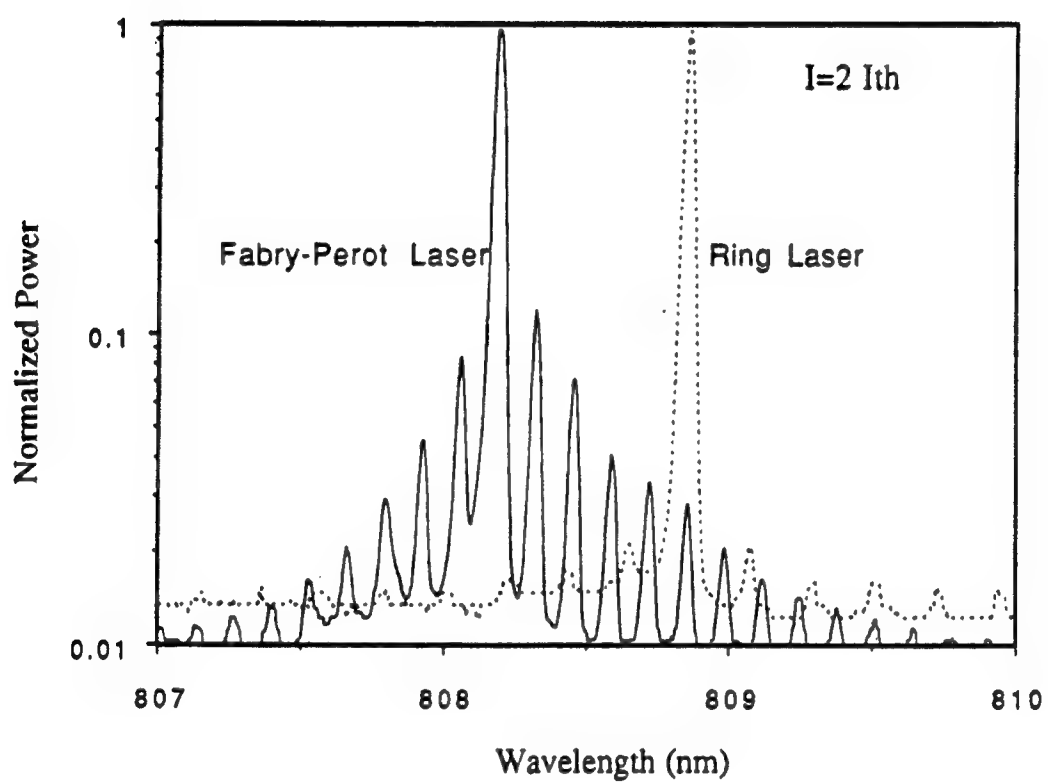
### Figure Captions

- Fig. 1 (a) SEM of the fabricated triangular ring laser. (b) Schematic drawing of the triangular ring cavity, with the structure angle defined.
- Fig. 2 Measured threshold current density of the ring lasers (right axis) and calculated  $\ln(1/R)$  (left axis) as a function of the structure angle.
- Fig. 3 Comparison of the spectrum of a Fabry-Perot laser (650  $\mu\text{m}$ ) and that of a ring laser (800  $\mu\text{m}$ ) at comparable injection currents.
- Fig. 4 Lateral far field of both a standard ring laser and a ring laser with EMR.
- Fig. 5 (a) Side-mode-suppression-ratio of a ring laser with EMR as a function of the injection current. (b) Spectrum of this ring laser at an injection current of 100 mA.

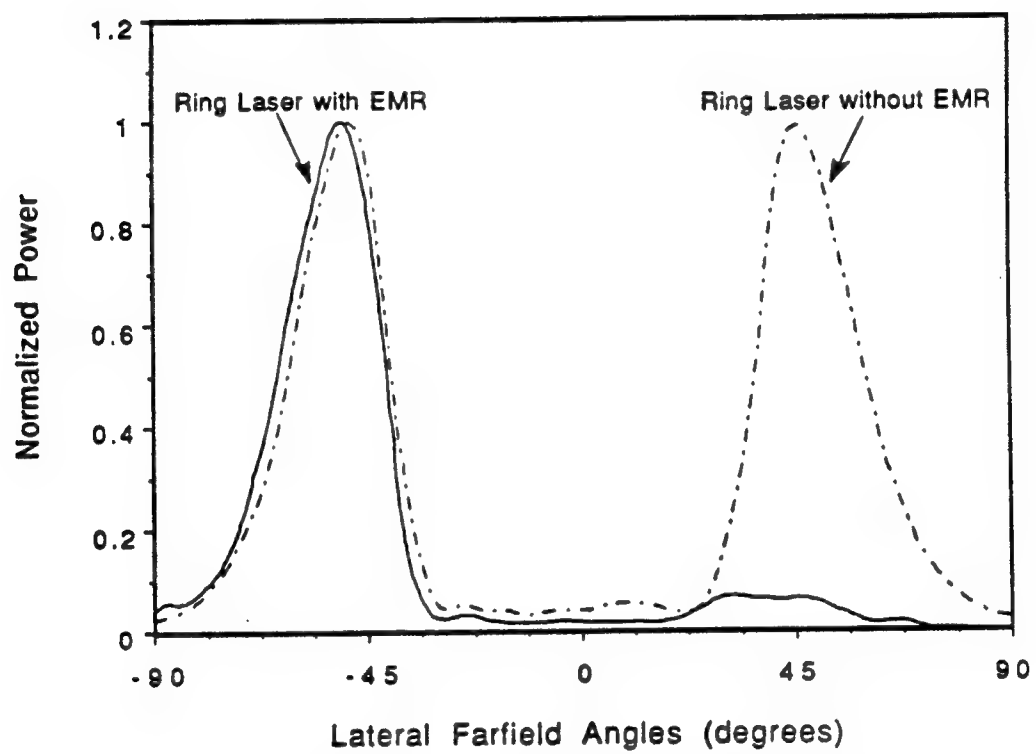


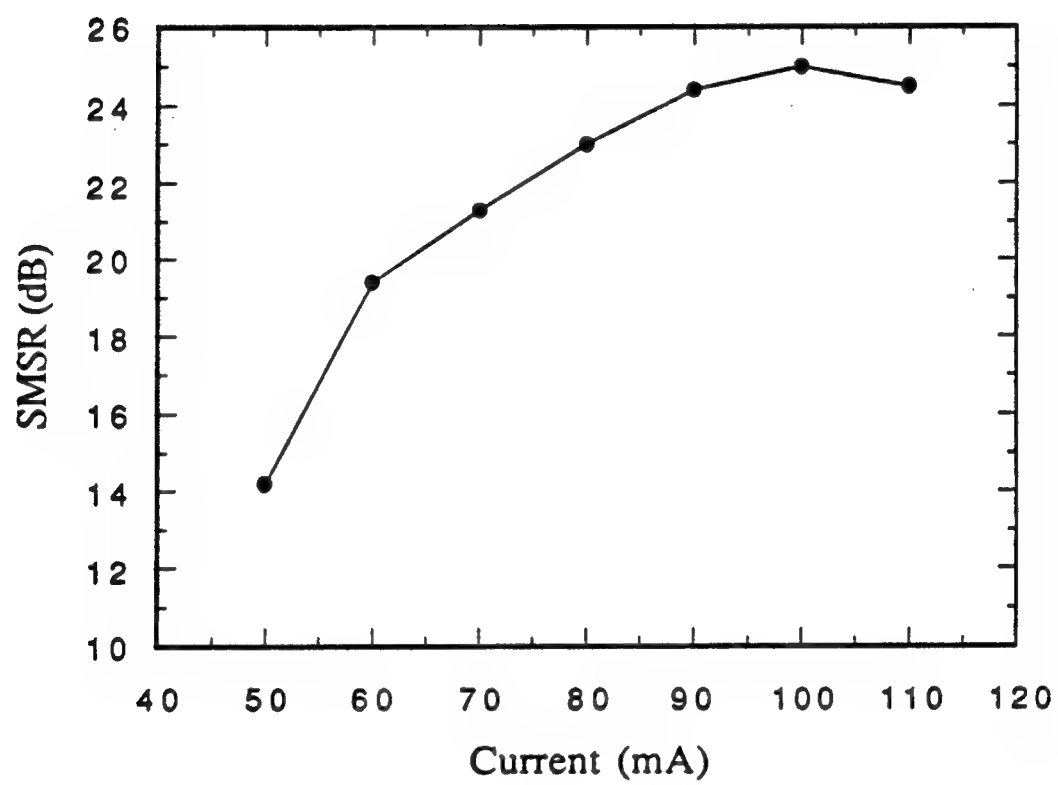


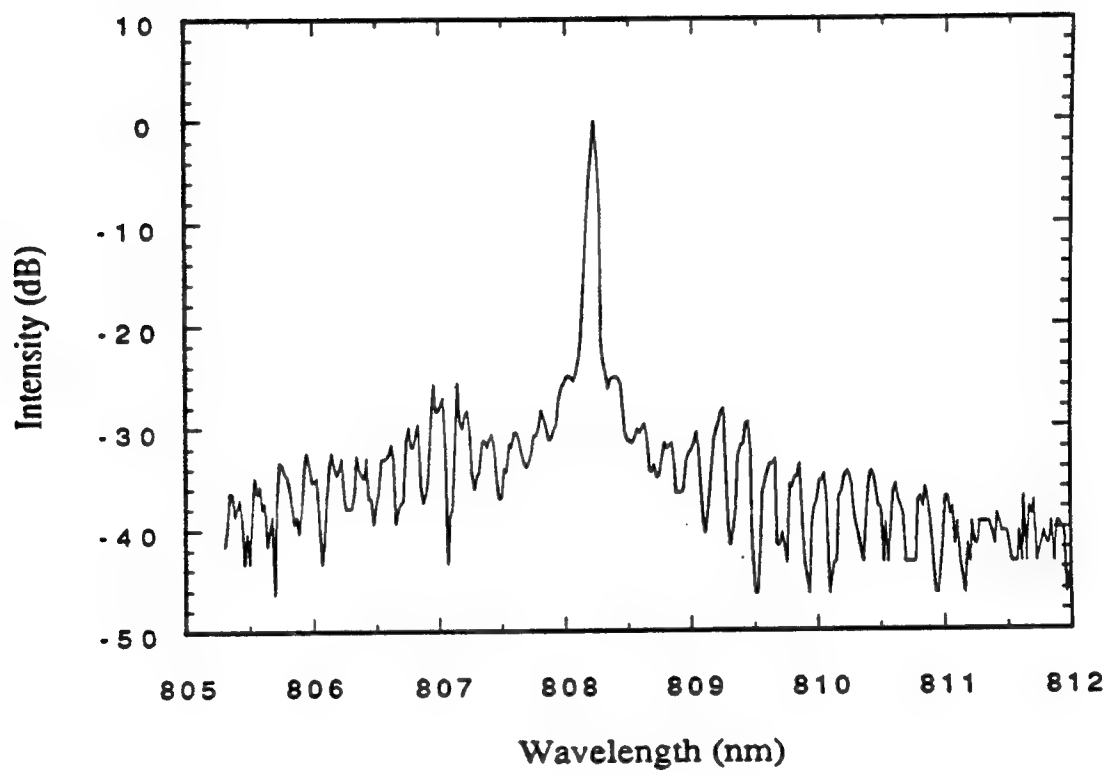












## **Self-Aligned V-shaped Lasers and Triangular Ring Lasers**

James J. Liang\*, Stanley T. Lau, Michael H. Leary, and Joseph M. Ballantyne

School of Electrical Engineering  
Cornell University  
Ithaca, NY 14853

\*Hewlett-Packard Company, 1040 NE Circle Blvd, Corvallis, Oregon 97330

### **ABSTRACT**

A self-aligned etching process is used, for the first time, to fabricate semiconductor ring lasers. V-shaped lasers with 90 degree turning mirrors are fabricated using the same self-aligned process. Very high reflectivity is achieved for the 90 degree turning mirrors. The dependencies of the ring laser threshold current and output power on the ring structure angle are demonstrated, consistent with the theoretical predictions. A power efficiency of 0.28 W/A is achieved for a ring laser with a structure angle of 10 degrees, which was the highest power efficiency reported for semiconductor ring lasers. A threshold current of 14 mA is achieved for a ring laser with a structure angle of 25 degrees, which was the lowest threshold current reported for single-lateral-mode semiconductor ring lasers. The ring lasers show much stronger tendency toward single-longitudinal-mode operation than the Fabry-Perot lasers fabricated on the same wafer. For some of the ring lasers, room-temperature continuous-wave (CW) operation was achieved without heat sinks.

# Self-Aligned V-shaped Lasers and Triangular Ring Lasers

## 1. Introduction

With the advancement of modern processing technology, semiconductor ring lasers are gaining popularity. In fact, a number of different ring cavity shapes have been reported, including triangular [1, 2], circular [3-6], oval [7], and square [8]. The triangular ring cavity consists of three straight waveguide sections meeting at three facets, two of which are high reflectivity mirrors with incidence angles beyond the critical angle, and one being the output facet. Among all the ring cavities, the triangular cavity has its unique advantages; these include its reduced size scale compared to the circular and oval cavities, its natural output coupling that none of the other ring cavities possesses, and most importantly, its unique versatility in the cavity design. We can engineer the threshold current and the output power of the triangular ring laser by simply adjusting its design parameter, namely the structure angle, which is defined as the incidence angle for the light at the output facet (or half of the vertex angle at the output facet). Adjusting the structure angle will change both the transmission (or output coupling) at the output facet and the effective reflectivity combining all three mirrors, and in turn vary the threshold current and the output power.

The laser material was an AlGaAs/GaAs graded index separate confinement heterostructure single quantum well (GRINSCH-SQW) grown by molecular beam epitaxy (MBE), with the quantum well being  $\text{Al}_{0.08}\text{Ga}_{0.92}\text{As}$ . Rectangular ridge lasers and V-shaped ridge lasers were

fabricated on the same wafer as the triangular ring lasers. A self-aligned process was used to fabricate the lasers, in which both the ridge waveguide and the facet pattern were defined by the same lithography step. Both the ridge waveguide and the facets were dry-etched using chemically assisted ion beam etching (CAIBE). The ridge waveguide was shallow etched stopping 0.1 micron above the active region for single-lateral-mode operation, while the facets were deep etched through the active region. 4.0 micron was used as the ridge width for all the lasers. The self-aligned dry-etching process is described in detail elsewhere [9]. While a self-aligned etching process has been used to fabricate optical turning mirrors [10-12], this is the first time that a self-aligned etching process has been used to fabricate semiconductor ring lasers.

In Section 2, we present the characteristics of the rectangular and V-shaped lasers, and the determination of the 90 degree turning mirror reflectivity. Section 3 discusses the triangular ring laser characteristics, and finally Section 4 summarizes the results.

## **2. Rectangular and V-shaped lasers**

The rectangular ridge laser is a standard Fabry-Perot laser with a ridge waveguide formed between two normal incidence mirrors. The V-shaped ridge laser consists of a ridge waveguide and three mirrors, two of which are normal incidence mirrors and the third mirror is a 90 degree optical turning mirror. Fig. 1 is the SEM of a fabricated V-shaped ridge

laser, and a close-up view of the 90 degree turning mirror is shown in Fig. 2. The etched mirror looks vertical and very smooth.

The lasers were tested under pulsed condition. The polarizations for both the rectangular ridge lasers and the V-shaped ridge lasers were found to be TE, parallel to the quantum well plane. Fig. 3 shows the visible image of a V-shaped laser under a probe and the infrared image of the same laser in action (with the background illumination turned off), as viewed from above under a microscope. The infrared lasing image of the V-shaped laser does not exhibit any noticeable scattered light from the 90 degree turning mirror, and a further examination of the digitized image shows that the integrated light intensity at the 90 degree turning mirror is only 1/40 of that at the normal incidence mirror, indicating very low scattering loss for the 90 degree turning mirror.

Shown in Fig. 4 is the measured threshold current density for both the rectangular lasers and the V-shaped lasers as a function of the inverse cavity length. The threshold current density for a standard Fabry-Perot laser is given by:

$$J_{th} = J_0 + (C/L) \ln(1/R) \quad (1)$$

where  $J_0$  is the current density required to achieve transparency and overcome losses other than mirror loss,  $C$  is a material constant,  $L$  is the cavity length, and  $R$  is the reflectivity for the normal incidence mirror.

Both  $J_0$  and  $C$  should be the same for all the lasers fabricated on the same wafer. The threshold current density for a V-shaped laser is given by:

$$J_{th} = J_0 + (C/L) \ln(1/RR^t) \quad (2)$$

where  $R$  is the reflectivity for the normal incidence mirror, and  $R^t$  is the 90 degree turning mirror reflectivity. Also shown in Fig. 4 is the straight fit for both the rectangular laser and V-shaped laser threshold current density, both lines intercept the y-axis at the same point, from which  $J_0$  is found to be 217 A/cm<sup>2</sup>. By taking the ratio of the two slopes for the straight lines,  $R^t$  is found to be related to  $R$  according to the following equation:

$$R^t = R^{0.1129} \quad (3)$$

Since the etched facets are very smooth, the reflectivity of the etched normal incidence mirror should be as good as that of a cleaved one. In fact, using a similar dry-etching technology, Behfar-Rad et al. [13] had shown that the reflectivity of an etched normal incidence facet was nearly identical to that of a cleaved one. Therefore, we can assume that the reflectivity for the etched normal incidence mirror  $R$  to be the same as that of a cleaved one, which is 0.32. From the slope of the rectangular laser line and assuming  $R=0.32$ ,  $C$  is determined to be 54.2 A/cm.

Using  $R=0.32$  in equation (3),  $R^t$  is found to be 88%, which was the highest 90 degree turning mirror reflectivity reported to date. This very high reflectivity is a consequence of both the smooth dry-etched facets which significantly reduces the scattering losses caused by facet



roughness and the self-aligned process which eliminates losses caused by facet displacement and lateral rotation. The theoretical limit for the 90 degree turning mirror reflectivity from a 3-D analysis [14] is about 95%, which indicates that the turning mirror had an additional scattering loss of only about 7%. This 7% loss should mostly come from residue facet roughness, because the verticality of the etched facets was very good. The turning mirror reflectivity  $R_t$  also varies very slowly with the etched normal incidence mirror reflectivity  $R$  according to equation (3). With  $R$  varying from 32% to 24%,  $R_t$  only changes from 88% to 85%.

There had been several previously reported results on the 90 degree dry-etched turning mirror reflectivity [8, 10-12, 15-17], with the best reflectivity achieved being 87% by Oku et al., for turning mirrors in a square InGaAs/AlGaAs ring laser operating at 1.02  $\mu\text{m}$  [8]. In our work, the lasing wavelength was 0.81  $\mu\text{m}$ . For the same facet roughness, the turning mirror reflectivity would be higher at longer wavelength, therefore the result in this work compares favorably with the result of Oku et al.

Shown in Fig. 5 is the pulsed spectrum of a rectangular laser with a cavity length of 700 micron biased at twice its threshold current, with the side-mode-suppression-ratio (SMSR) being about 6 dB.

### 3. Triangular ring lasers

Ring lasers with various cavity length and structure angles were fabricated. Shown in Fig. 6 and Fig. 7 are the SEM pictures of fabricated

ring lasers with structure angles of 8° and 25° respectively. The ring lasers were first tested under pulsed condition.

In order to investigate the dependence of the laser characteristics on the structure angle, ring lasers with a fixed cavity length of 600 μm, but with varying structure angles from 6° to 25° were fabricated. The polarization for these ring lasers were found to be predominantly TE parallel to the quantum well plane. Fig. 8 shows the measured threshold current of these ring lasers as a function of the structure angle, with the 0° structure angle data taken from a rectangular laser with a cavity length of 600 μm. The threshold current density  $J_{th}$  for the ring lasers is given by:

$$J_{th} = J_0 + (C/L) \ln(1/R_{eff}) \quad (4)$$

where  $R_{eff}$  is equal to  $R_1 R_2 R_3$ , which is the effective reflectivity combining all three mirrors. From the measured threshold current, the threshold current density  $J_{th}$  can be determined. Using  $J_0 = 217 \text{ A/cm}^2$ ,  $C = 54.2 \text{ A/cm}$ , and equation (4), the experimental effective reflectivity  $R_{eff}$  can also be determined. Shown in Fig. 9 is the experimentally determined effective reflectivity as a function of the structure angle, as well as the theoretically calculated effective reflectivity for TE modes from the 3-D analysis [14]. The experimentally determined reflectivities follow the theoretical trend fairly well. There also appears to be a small overall shift between the experimental reflectivities and the calculated ones due to residue facet roughness. The small shift for structure angles beyond the critical angle accounts for an additional scattering loss of only about 6% for each of the three mirrors. This agrees well with the 7%

additional loss from facet roughness for the 90 degree turning mirror, as discussed in Section 2.

As seen from Fig. 8, as the structure angle is increased beyond the critical angle ( $\sim 18^\circ$ ), the threshold currents of the ring lasers are significantly reduced as compared with the rectangular lasers. This demonstrates the low threshold potential of the ring lasers. Fig. 10 shows the light-current characteristics of a ring laser with a cavity length of  $300\text{ }\mu\text{m}$  and a structure angle of  $25^\circ$ . The threshold current of this laser was 14 mA, which was the lowest threshold current reported to date for single-lateral-mode semiconductor ring lasers. This was an order of magnitude improvement from previously reported single-mode triangular ring laser [18], and single-mode circular ring laser [6].

The ring lasers displayed two output beams, one from the clockwise circulating direction, and the other from the counter-clockwise direction. Shown in Fig. 11 is the measured output power combining both beams of these ring lasers as a function of the structure angle with each laser biased at twice its threshold current. The measured power was the total output from both beams. Again the  $0^\circ$  structure angle data was taken from a rectangular laser with the same cavity length ( $600\text{ }\mu\text{m}$ ) as the ring lasers and the power was the total from both facets. Fig. 12 is the transmission (output coupling) as a function of the structure angle for both the TE and TM modes, calculated from the 3-D analysis [6]. As seen from Fig. 11, the dependence of the output power on the structure angle follows fairly well the same trend as the theoretically calculated output coupling for TE modes, with some small deviations possibly caused by

material non-uniformity. For small structure angles (less than  $\sim 14^\circ$ ), the ring lasers show comparable output powers as the rectangular lasers (but much improved spectra). Fig. 13 is the light-current characteristics of a ring laser with a cavity length of  $600\text{ }\mu\text{m}$  and a structure angle of  $10^\circ$ , with the output power being the combination of the two beams. The slope efficiency for this laser was found to be  $0.28\text{ W/A}$ , which was the highest slope efficiency reported to date for semiconductor ring lasers. This high slope efficiency is a direct consequence of the unique cavity structure of the triangular ring lasers. The triangular ring provides a natural and the most efficient way of output coupling among all the ring cavities, because the light can come out directly from the output facet with an adjustable incidence angle. The circular and oval rings, on the other hand, have to couple the internally circulating light out by fabricating additional couplers, like Y-junction couplers [4, 5, 7], which results in substantial loss of power at the junctions. The square ring laser, with four totally reflecting facets, would have to couple the light out by evanescent coupling [8], which will result in very low coupling efficiency.

The spectral characteristics for the ring lasers were measured and the ring lasers showed much stronger tendency toward single-longitudinal-mode operation than the Fabry-Perot laser fabricated on the same wafer. Shown in Fig. 14 is the measured spectra for a ring laser with a cavity length of  $800\text{ }\mu\text{m}$  and a structure angle of  $16^\circ$ , biased at twice its threshold current. The SMSR was about 17 dB, compared to 6 dB for the rectangular laser shown in Fig. 5.

The longitudinal mode spacing for a ring laser is given by [19]:

$$\Delta\lambda = 2\lambda^0 / (n_g L) \quad (5)$$

where  $L$  is the cavity length of the ring laser,  $n_g$  is the group index of refraction, and  $\lambda^0$  is the free-space lasing wavelength. A ring laser has twice the mode spacing of a Fabry-Perot laser with the same cavity length, due to the fact that in a Fabry-Perot cavity the light travels back and forth through the cavity twice in one round trip; while in a ring cavity the light goes through the cavity only once in one round trip. Shown in Fig. 15 is the measured longitudinal mode spacing for the ring lasers as a function of the inverse cavity length, with those of the rectangular lasers also shown for comparison. Using  $\lambda^0 = 0.81$  micron,  $n_g$  is determined to be 3.78 from the slope of the line. The ring laser slope is found to be twice the rectangular laser one as expected.

The ring lasers were also tested under continuous-wave (CW) conditions at room temperature unbonded to any heat sinks. While some of the ring lasers showed considerable power saturation as the injection current was increased above the threshold, there were some ring lasers that displayed good light-current characteristics. Shown in Fig. 16 is the light-current characteristics of a ring laser under both pulsed and CW conditions, with the power being the combination of both output beams. The ring cavity length was 800  $\mu\text{m}$ , and the structure angle was  $12^\circ$ .

#### **4. Summary**

A self-aligned dry-etching process was used, for the first time, to fabricate semiconductor ring lasers. Rectangular lasers, V-shaped lasers, and triangular ring lasers were fabricated on the same wafer. Very high reflectivity was achieved for the 90 degree turning mirror for the V-shaped lasers. The threshold current and the output power dependencies on the ring structure angle were demonstrated, consistent with theoretical calculations. This was the first demonstration of a laser cavity in which both the threshold current and the output power can be controlled by geometry alone. A slope efficiency of 0.28 W/A was observed for a ring laser with a structure angle of  $10^\circ$ , a cavity length of 600  $\mu\text{m}$ , and a ridge width of 4  $\mu\text{m}$ , which was the highest slope efficiency ever reported for semiconductor ring lasers. For a ring laser with a cavity length of 300  $\mu\text{m}$ , a ridge width of 4  $\mu\text{m}$ , and a structure angle of  $25^\circ$ , a threshold current of 14 mA was achieved, the lowest reported for single-lateral-mode semiconductor ring lasers. The ring lasers showed much stronger tendency toward single-longitudinal-mode operation than the Fabry-Perot lasers fabricated on the same wafer. CW operation was demonstrated for the triangular ring laser at room temperature without any heat sinks.

#### **ACKNOWLEDGMENTS**

This work was funded by the Air Force and ARPA under Rome Laboratory Contract No. F30602-92-C-0082 and General Electric (now

Martin Marietta). All fabrication was performed at the National Nanofabrication Facility which is supported by the National Science Foundation, Cornell University, and industrial affiliates. We would like to thank Dr. A. Behfar-Rad for fruitful discussions.

## REFERENCES

- [1] A. Behfar-Rad, S.S. Wong, and J.M. Ballantyne, "Traveling-wave operation in a triangular-shaped monolithic semiconductor ring ridge laser," *Proc. IEDM*, vol. 6(8), pp. 1, 1990.
- [2] A. Behfar-Rad, S.S. Wong, and J.M. Ballantyne, "AlGaAs/GaAs-based triangular-shaped ring ridge lasers," *Appl. Phys. Lett.*, vol. 60, pp. 1658-1660, 1992.
- [3] T. Krauss, P.J.R. Laybourn, and J. Roberts, "CW operation of semiconductor ring lasers," *Electron. Lett.*, vol. 26, pp. 2095-2097, 1990.
- [4] H. Han, M.E. Favaro, D.V. Forbes, and J.J. Coleman, "In<sub>x</sub>Ga<sub>1-x</sub>As-Al<sub>y</sub>Ga<sub>1-y</sub>As-GaAs strained layer quantum well heterostructure circular ring lasers," *IEEE Photon. Technol. Lett.*, vol. 4, pp. 817-819, 1992.
- [5] J.P. Hohimer, D.C. Craft, G.R. Hadley, G.A. Vawter, and M.E. Warren, "Single frequency continuous wave operation of ring resonator diode lasers," *Appl. Phys. Lett.*, vol. 59, pp. 3360-3362, 1991.
- [6] P.B. Hansen, G. Raybon, M.-D. Chien, U. Koren, B.I. Miller, M.G. Young, J.-M. Verdiell, and C.A. Burrus, "A 1.54  $\mu$ m monolithic semiconductor ring laser: CW and mode locked operation," *IEEE Photon. Technol. Lett.*, vol. 4, pp. 411-413, 1992.
- [7] J.P. Hohimer, G.A. Vawter, and D.C. Craft, "Unidirectional semiconductor ring lasers," *Technical Digest of CLEO'93*, pp. 266-267, 1993.



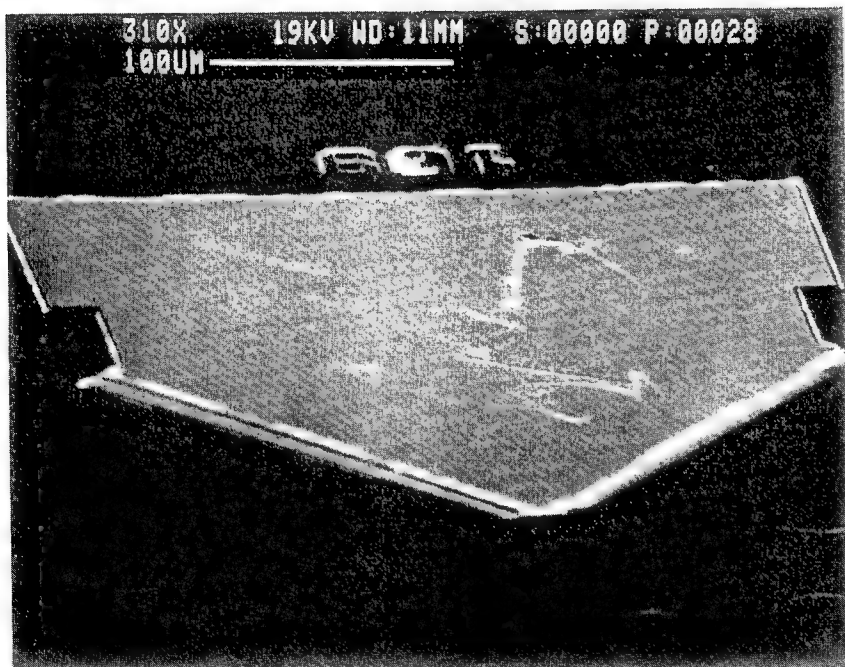
- [8] S. Oku, M. Okayasu, and M. Ikeda, "Low threshold CW operation of square-shaped semiconductor ring lasers," *IEEE Photon. Technol. Lett.*, vol. 3, pp. 588-590, 1991.
- [9] J.J. Liang, and J.M. Ballantyne, "Self-aligned dry-etching process for waveguide diode ring lasers," *J. Vac. Sci. Technol. B*, vol. 12, pp. 2929-2932, 1994.
- [10] H. Appelman, J. Levy, M. Pion, D. Krebs, C. Harding, and M. Zediker, "Self-aligned chemically assisted ion beam etched GaAs/AlGaAs turning mirrors for photonic applications," *J. Lightwave Technol.*, vol. 8, pp. 39-41, 1990.
- [11] E. Gini, G. Guekos, and H. Melchior, "Low loss corner mirrors with 45 degree deflection angle for integrated optics," *Electron. Lett.*, vol. 28, pp. 499-501, 1992.
- [12] J.E. Johnson, and C.L. Tang, "Precise determination of turning mirror loss using GaAs/AlGaAs lasers with up to ten 90 degree intracavity turning mirrors," *IEEE Photon. Technol. Lett.*, vol. 4, pp. 24-26, 1992.
- [13] A. Behfar-Rad, S.S. Wong, and J.M. Ballantyne, B.A. Soltz, and C.M. Harding, "Rectangular and L-shaped GaAs/AlGaAs lasers with very high quality etched facets," *Appl. Phys. Lett.*, vol. 54, pp. 493-495, 1989.
- [14] S.T. Lau, and J.M. Ballantyne, "2-D analysis of a dielectric waveguide mirror," *Conference Proceedings of LEOS'94*, vol. 2, pp.55-56, 1994.
- [15] P. Buchmann, and H. Kaufmann, "GaAs single-mode rib waveguides with reactive ion-etched totally reflecting corner mirrors," *J. Lightwave Technol.*, vol. 3, pp. 785-788, 1985.

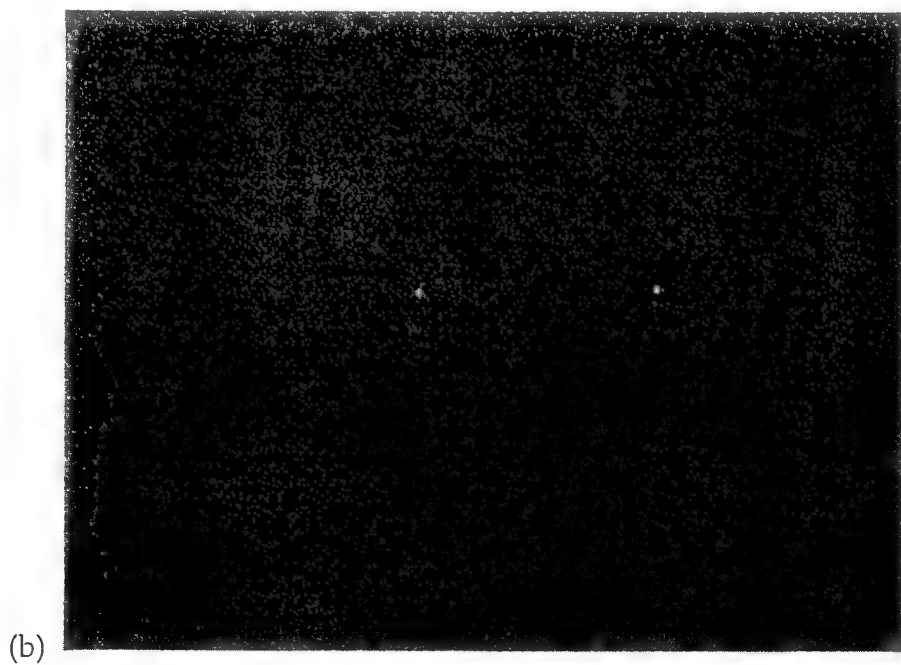
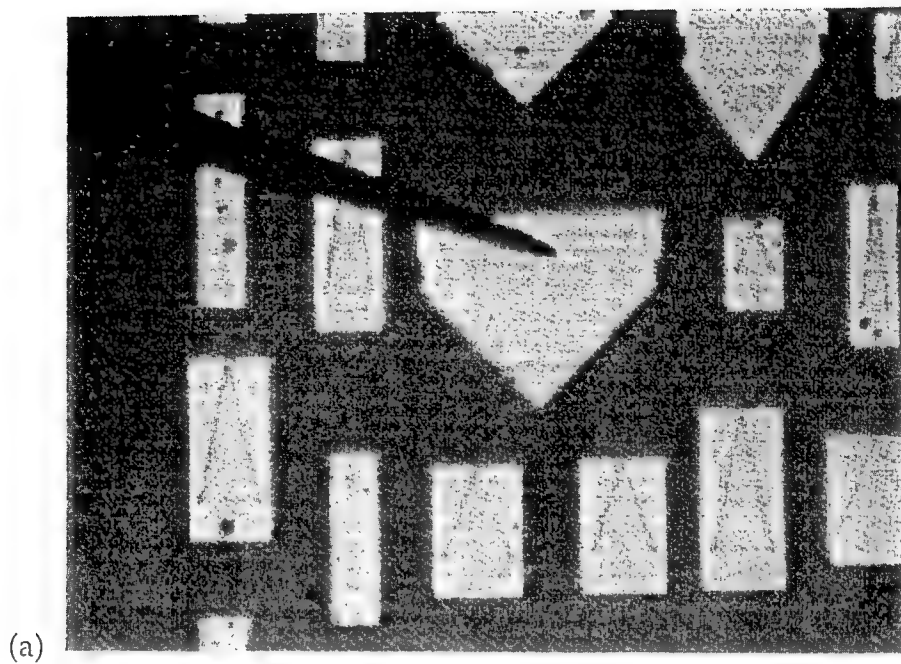
- [16] F. Shimokawa, H. Tanaka, R. Sawada, and S. Hara, "Continuous-wave operation and mirror loss of a U-shaped GaAs/AlGaAs laser diode with two totally reflecting mirrors," *Appl. Phys. Lett.*, vol. 56, pp. 1617-1619, 1990.
- [17] R. van Roijen, G.L.A. van der Hofstad, M. Groten, J.M.M. van der Heyden, P.J.A. Thijs, and B.H. Verbeek, "Fabrication of low-loss integrated optical corner mirrors," *Appl. Optics*, vol. 32, pp. 3246-3248, 1993.
- [18] A. Behfar-Rad, " Novel semiconductor laser structure fabricated with chemically assisted ion beam etching," Ph.D. Thesis, Cornell University, Ithaca, New York, 1990.
- [19] J.R. Wilkinson, "Ring Lasers," in "Progress in Quantum Electronics," vol. 11-12, pp. 24, 1987/88.

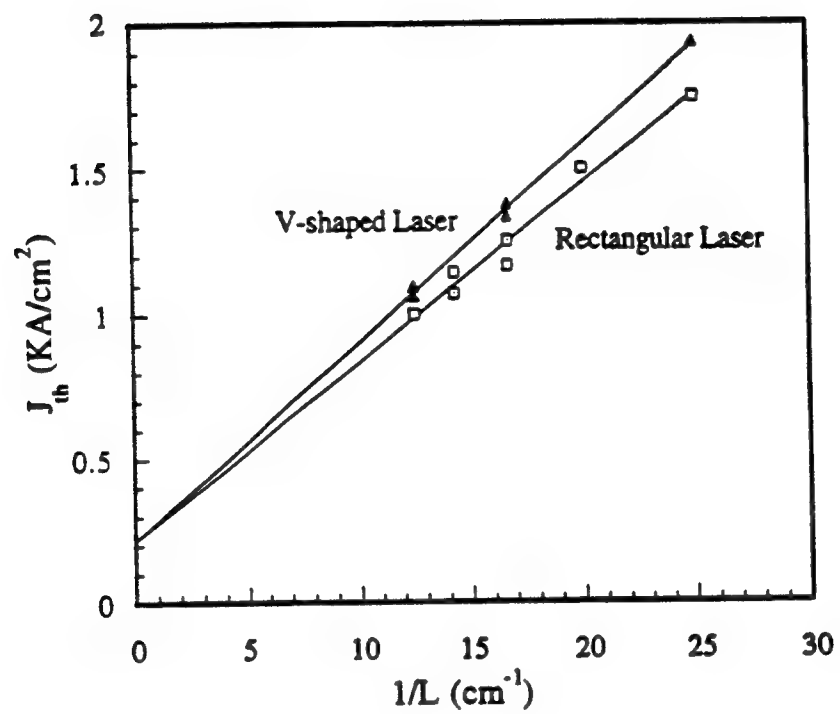
## Figure Captions

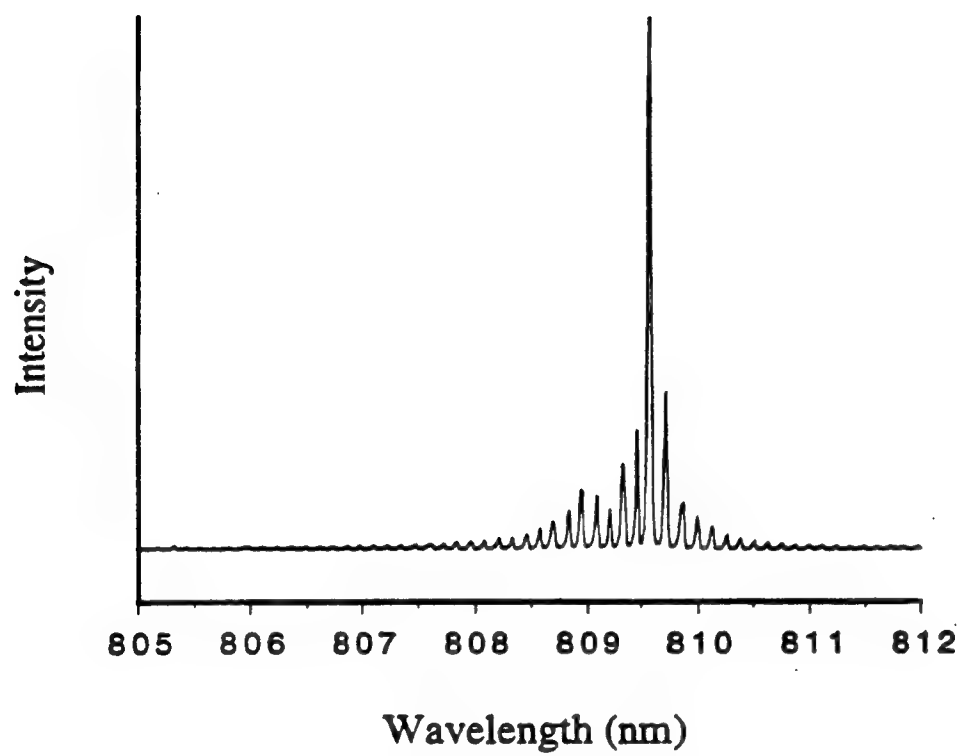
- Fig. 1 SEM of a fabricated V-shaped laser.
- Fig. 2 SEM of the 90 degree turning mirror for the V-shaped laser.
- Fig. 3 (a) Visible image and (b) infrared lasing image of a V-shaped laser, viewed from above under a microscope.
- Fig. 4 The threshold current density for both the rectangular lasers and the V-shaped lasers, as a function of the inverse cavity length.
- Fig. 5 The spectrum of a rectangular laser with a cavity length of 700  $\mu\text{m}$  biased at twice its threshold current.
- Fig. 6 SEM of a ring laser with a structure angle of  $8^\circ$ .
- Fig. 7 SEM of a ring laser with a structure angle of  $25^\circ$ .
- Fig. 8 The measured threshold current of ring lasers with fixed cavity length of 600  $\mu\text{m}$  as a function of the structure angle.
- Fig. 9 The experimental and calculated effective reflectivity combining all three mirrors for the ring lasers as a function of the structure angle.

- Fig. 10 Pulsed light-current characteristics of a ring laser with a cavity length of 300  $\mu\text{m}$  and a structure angle of  $25^\circ$ .
- Fig. 11 The experimental output power combining both beams for ring lasers with fixed cavity length of 600  $\mu\text{m}$  as a function of the structure angle, with each laser biased at twice its threshold current.
- Fig. 12 3-D calculation of the output coupling for both the TE and TM modes as a function of the structure angle for the ring laser.
- Fig. 13 Pulsed light-current characteristics of a ring laser with a cavity length of 600  $\mu\text{m}$  and a structure angle of  $10^\circ$ , with the power being the total of the two output beams.
- Fig. 14 The spectrum of a ring laser with a cavity length of 800  $\mu\text{m}$  and a structure angle of  $16^\circ$  biased at twice of its threshold current.
- Fig. 15 The longitudinal mode spacing as a function of the inverse cavity length for both the ring lasers and the rectangular lasers.
- Fig. 16 The light-current characteristics under both pulsed and CW conditions, of a ring laser with a cavity length of 800  $\mu\text{m}$  and a structure angle of  $12^\circ$ .

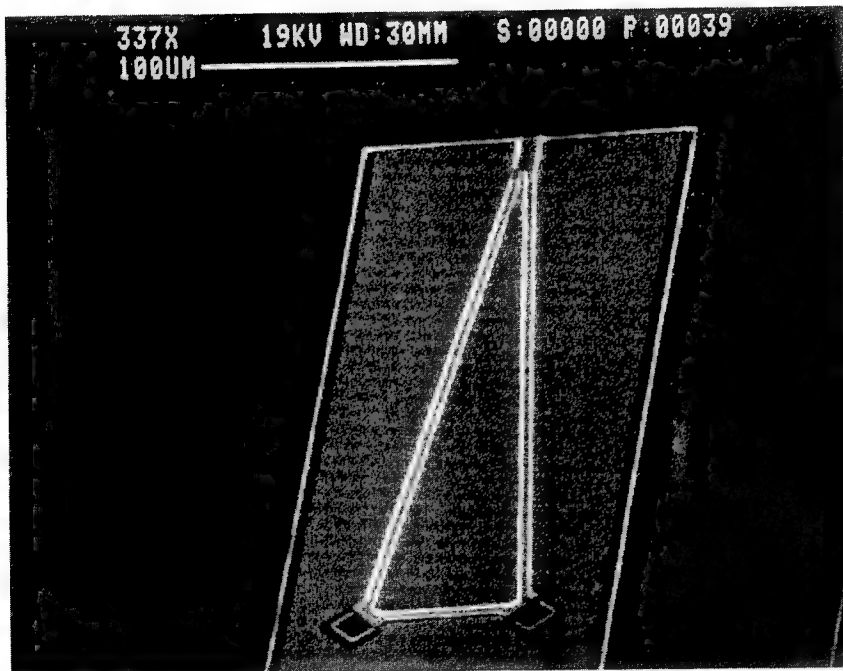


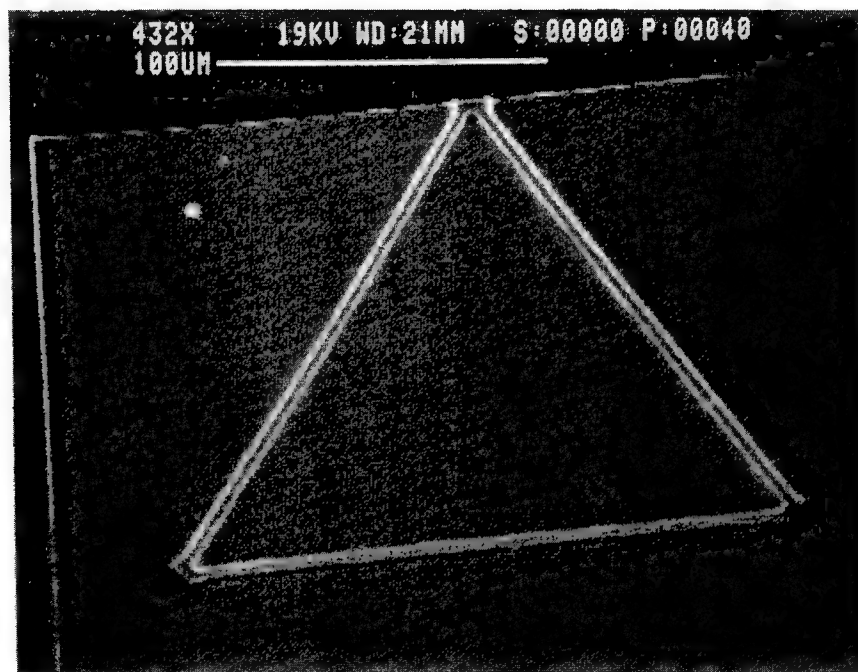


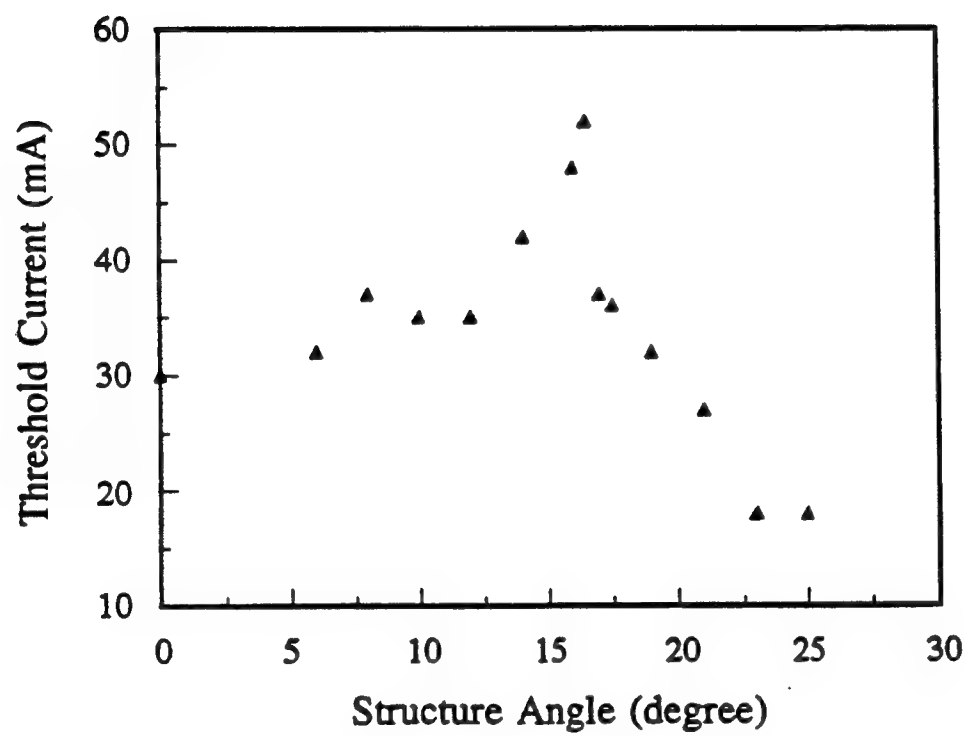


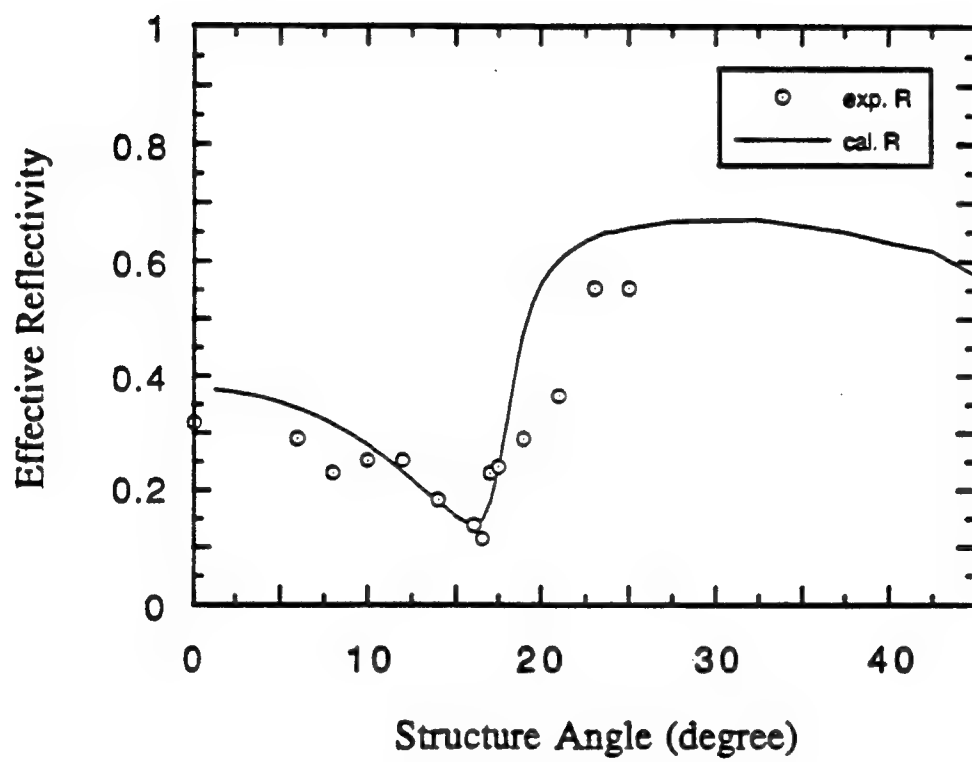


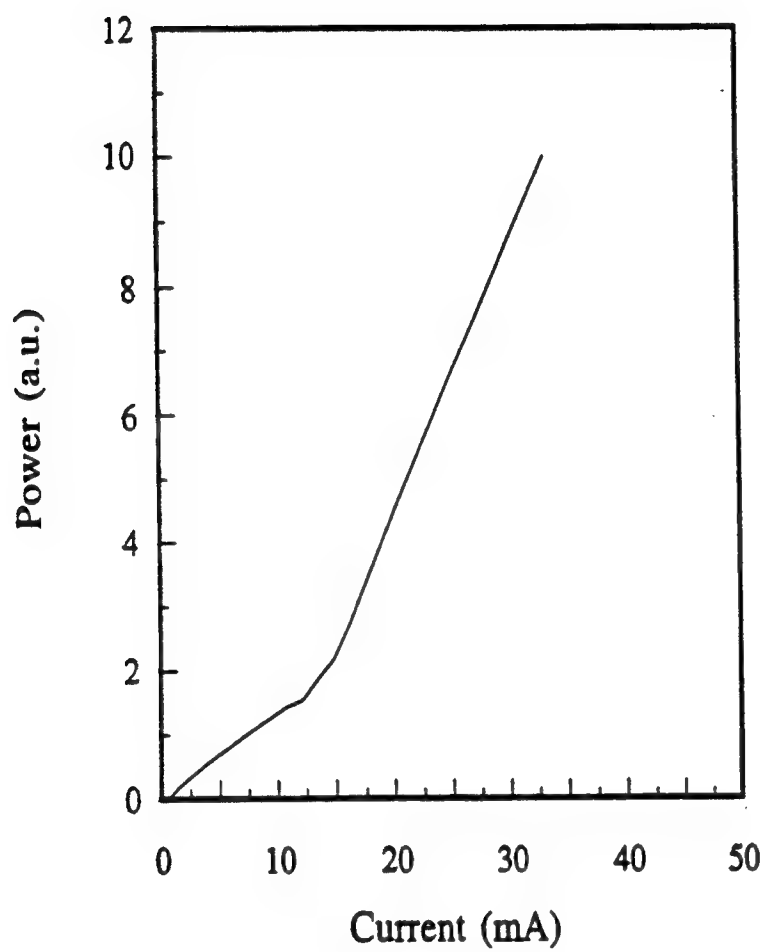


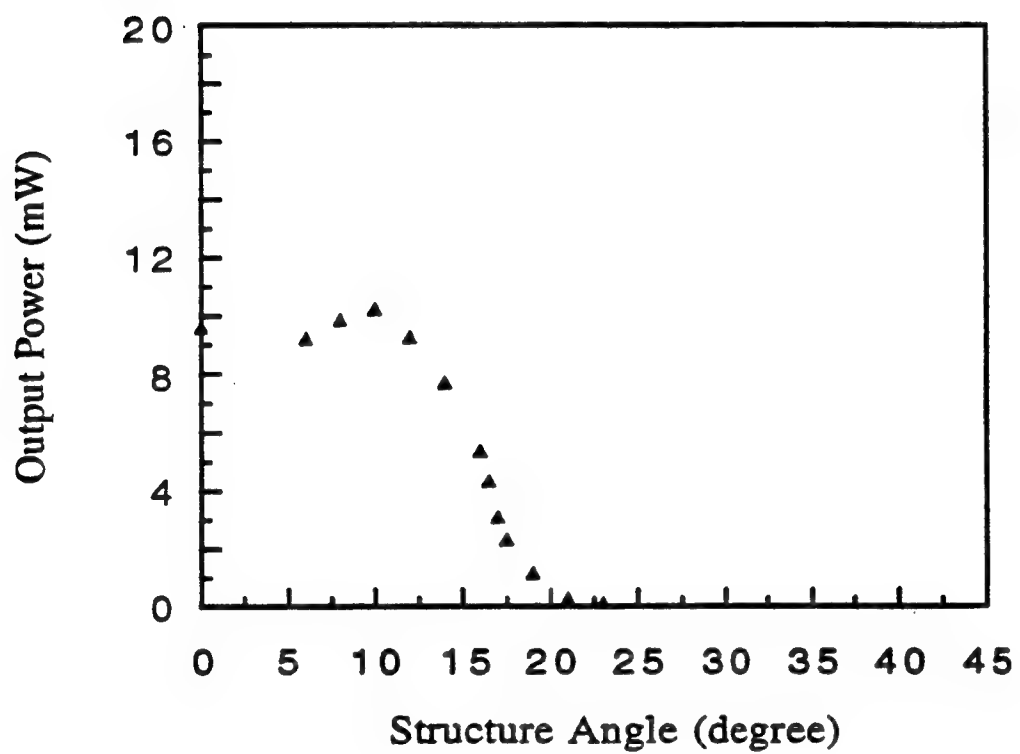


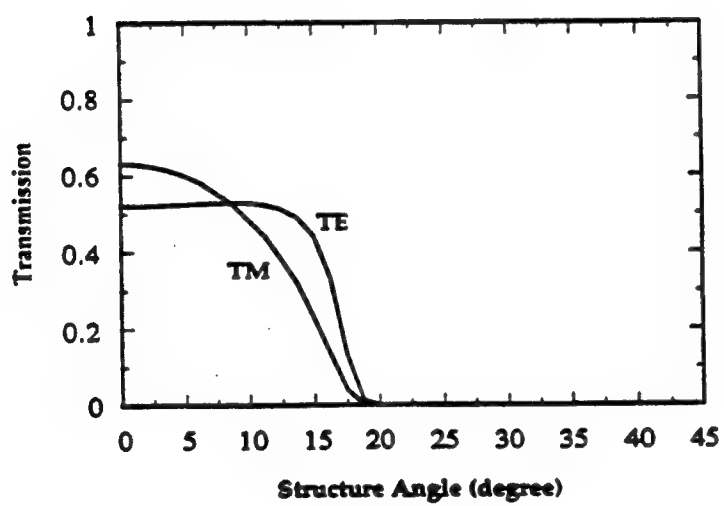


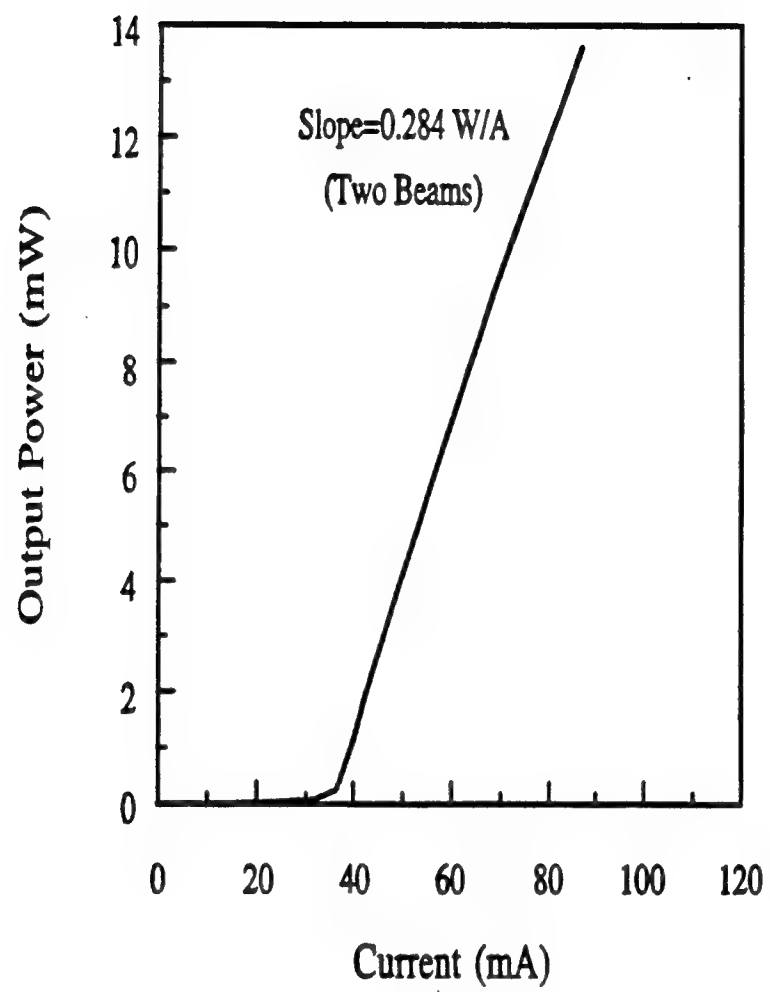




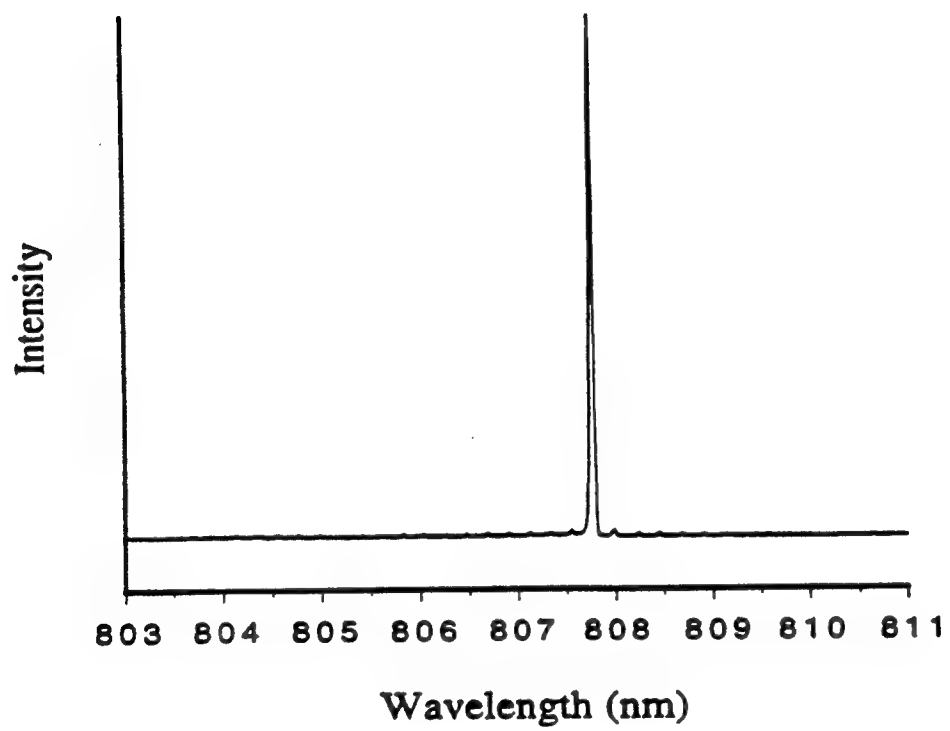


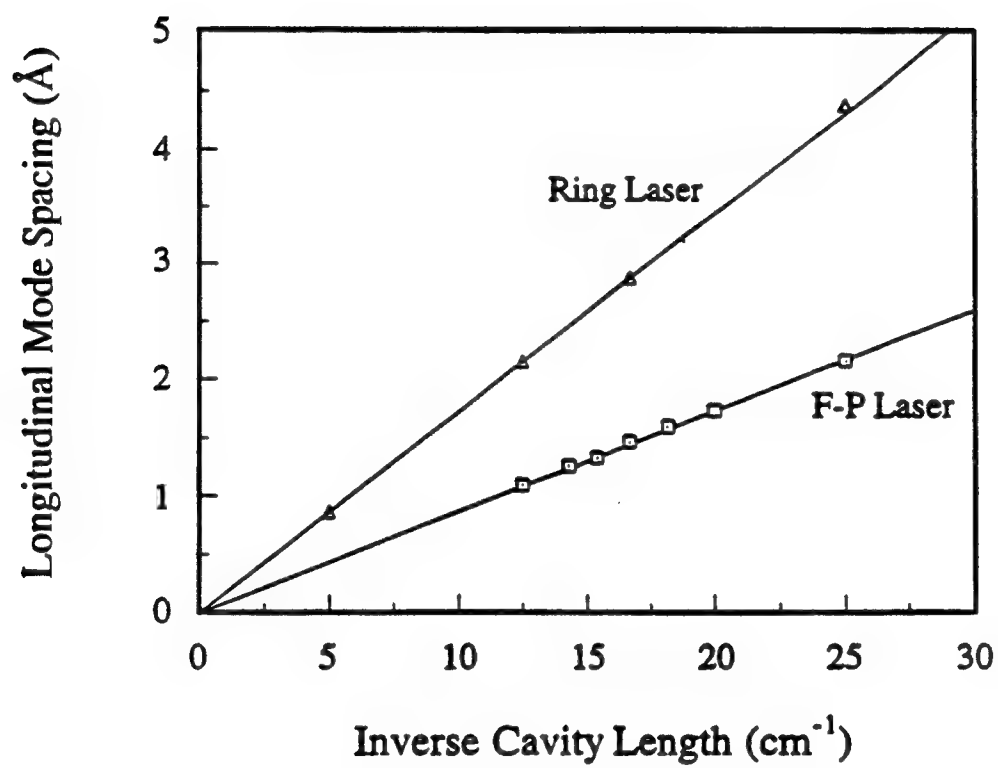


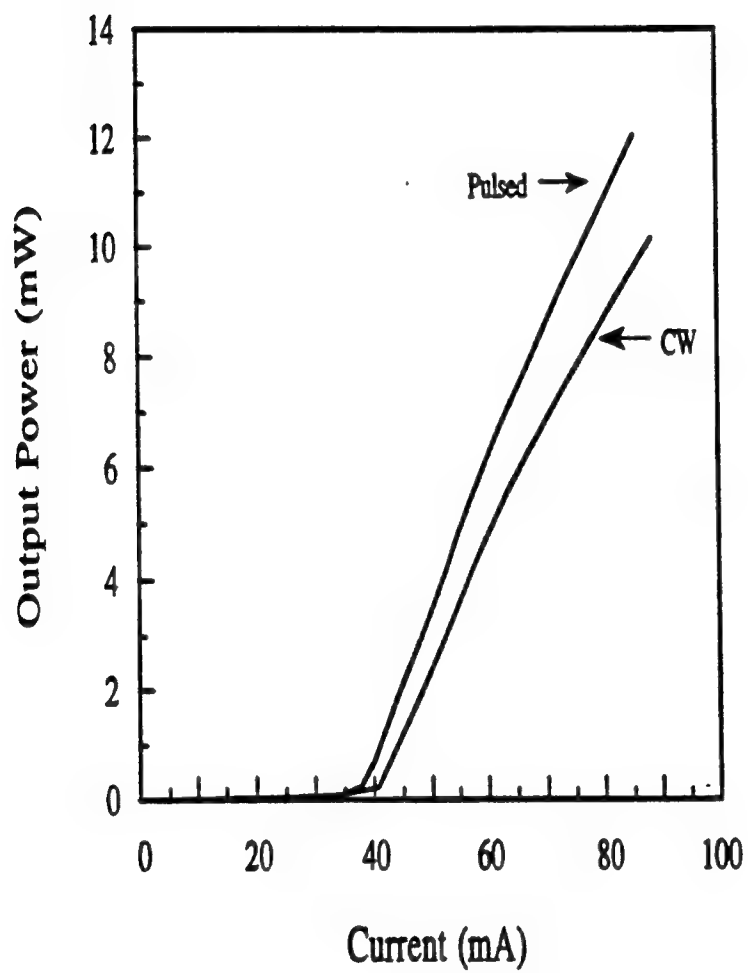












APPENDIX 4

**Unidirectional Operation of Waveguide Diode Ring Lasers**

James J. Liang\*, Stanley T. Lau, Mike H. Leary, and Joseph M. Ballantyne

School of Electrical Engineering,  
Cornell University,  
Ithaca, NY 14853

\*Hewlett-Packard Company, 1040 NE Circle Blvd, Corvallis, OR 97330

**ABSTRACT**

A novel method of providing asymmetric feedback in the triangular ring laser structure was devised through the simple alterations of the waveguide shape. Two kinds of alterations were designed and implemented, one being the "optical diode", the other being the tapered waveguide. Unidirectional operation was achieved for the ring lasers, with a single-beam slope efficiency of 0.23 W/A, which was the highest single-beam slope efficiency reported for semiconductor ring lasers.

## Unidirectional Operation of Waveguide Diode Ring Lasers

Unidirectional operation of semiconductor ring lasers is desired because it offers the advantages of enhanced mode purity and higher single beam power. In order to achieve unidirectional operation, a non-reciprocal element has to be implemented in the ring laser structure that favors one circulating direction over the other. Using a scattering matrix analysis, Lau et al. [1] found that the two internal powers became asymmetric if a preferential cross coupling of the two circulating directions was introduced. The direction that receives stronger cross coupling than the other would become the dominant beam. In fact, unidirectional operation has been reported for both the square ring lasers [2] and the circular ring lasers [3] by providing preferential cross coupling for one circulating direction over the other. This paper reports a novel method of providing preferential cross coupling through simple alterations of the waveguide shape.

The ring lasers were triangular-shaped, with two totally reflecting facets and one output facet, [4, 5] The epitaxial layer was an AlGaAs/GaAs graded index separate confinement heterostructure single quantum well (GRINSCH-SQW) grown by molecular beam epitaxy (MBE), with the quantum well being  $\text{Al}_{0.08}\text{Ga}_{0.94}\text{As}$ . The ring lasers were fabricated using a self-aligned dry-etching process, [6] with the facets deep etched and the ridge waveguide shallow etched allowing single-lateral-mode operation. There were two kinds of alterations designed for the ring lasers, the first is the "optical diode" and shown in Fig. 1. The "optical diode" was designed so that it consists of a tapering section that widens the waveguide very

gradually followed by an abrupt section that narrows the waveguide to the original width. This structure would provide preferential cross coupling into the clockwise circulating direction, because the counter-clockwise circulating light arrives at the gradual tapering section first, at which the lateral mode would slowly expand as the ridge width widens, and when the abrupt section is reached, some light would be reflected back into the clockwise direction as a result of the sudden narrowing of the waveguide width. As a result, the clockwise circulating direction receives more cross coupling than the counter-clockwise direction. Therefore, this structure acts like an optical diode, favoring the circulating direction toward which the diode is pointing (the clockwise direction). The other alteration was the tapered waveguide shown in Fig. 2, which would also favor the clockwise direction because the counter-clockwise circulating light suffers from a larger loss at the bottom right turning mirror. When the counter-clockwise circulating light arrives at the bottom right mirror with a widened mode, some of the light would miss the turning mirror and result in larger losses than the clockwise direction.

Fig. 3 shows the lateral far field of a ring laser with an optical diode (as shown in Fig. 1) at twice its threshold current. The ring cavity length was 800  $\mu\text{m}$ , the structure angle (the incidence angle at the output facet) was  $12^\circ$ , and the ridge width was 4  $\mu\text{m}$ . As expected, the output beam from the clockwise circulating direction, which is plotted on the left-hand in Fig. 3, was the dominant beam, with the peak intensity ratio between the clockwise beam and counter-clockwise beam being 20 to 1. Shown in Fig. 4 is the pulsed light-current characteristics of this ring laser for the dominant clockwise beam, with a single-beam slope

efficiency of 0.23 W/A achieved, which is to our knowledge the highest single-beam slope efficiency reported to date for semiconductor ring lasers. The two-beam slope efficiency for a standard bidirectional ring laser with the same cavity length, ridge width and structure angle was found to be 0.26 W/A. The closeness of the single-beam slope efficiency to the two-beam slope efficiency indicates that the majority of the power for the ring laser with the optical diode is now concentrated in one circulating direction only, which further confirms its unidirectional operation.

Shown in Fig. 5 is the CW log-spectrum of this unidirectional ring, as well as those of a rectangular laser with a cavity length of 700  $\mu\text{m}$  and a standard bidirectional ring with a cavity length of 800  $\mu\text{m}$  and a structure angle of  $12^\circ$ . All three lasers were biased at twice their threshold current. The SMSR for the rectangular laser was about 4 dB, while that of the bidirectional ring was improved to about 17 dB and that of the unidirectional ring was further improved to about 22 dB.

Fig. 6 is the lateral far field of a ring laser with a tapered waveguide as shown in Fig. 2 at twice its threshold current. The ring cavity length was 600  $\mu\text{m}$ , and the structure angle was  $12^\circ$ . The clockwise beam was found to be the dominant one as expected, with the peak intensity ratio between the two output beams being 33 to 1.

In conclusion, a novel method of providing asymmetric feedback in the ring laser structure is devised, through the simple alterations of the waveguide shape. A peak intensity ratio of 20 to 1 was observed for a ring

laser with an optical diode, with a single beam slope efficiency of 0.23 W/A, which was the highest single-beam slope efficiency reported to date for semiconductor ring lasers. The ring laser with the optical diode showed improvement in the SMSR over the standard bidirectional ring lasers. The implementation of the tapered waveguide resulted in a peak intensity ratio of 33 to 1.

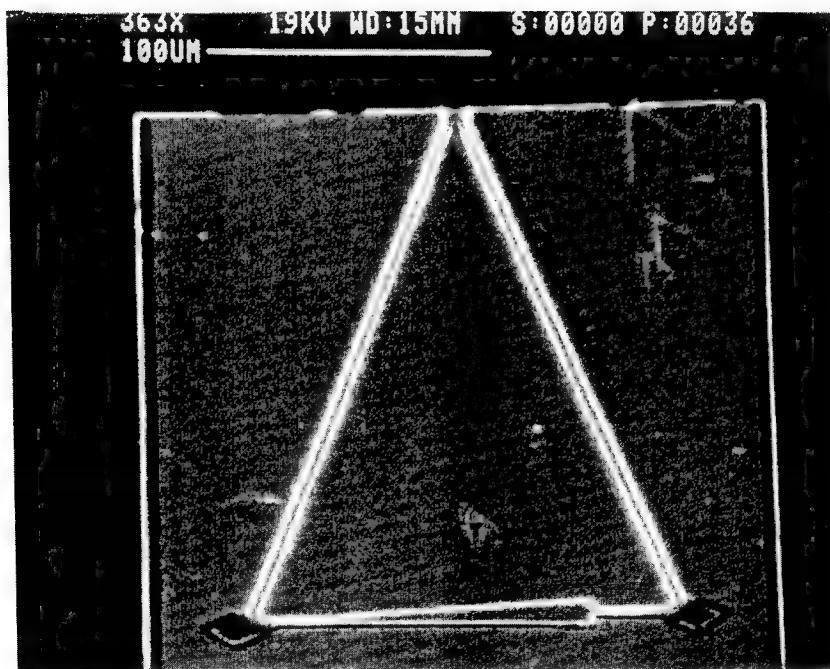


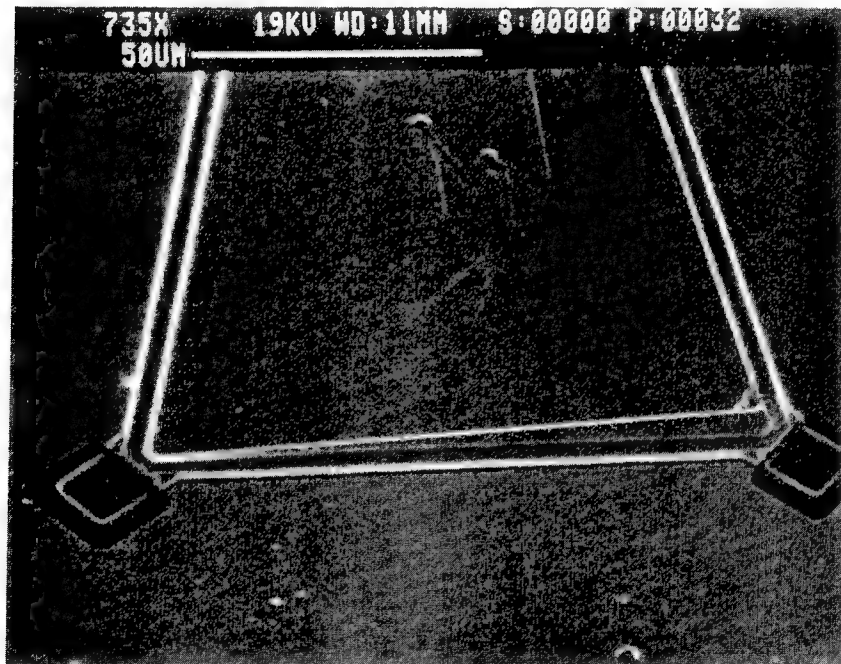
## REFERENCES

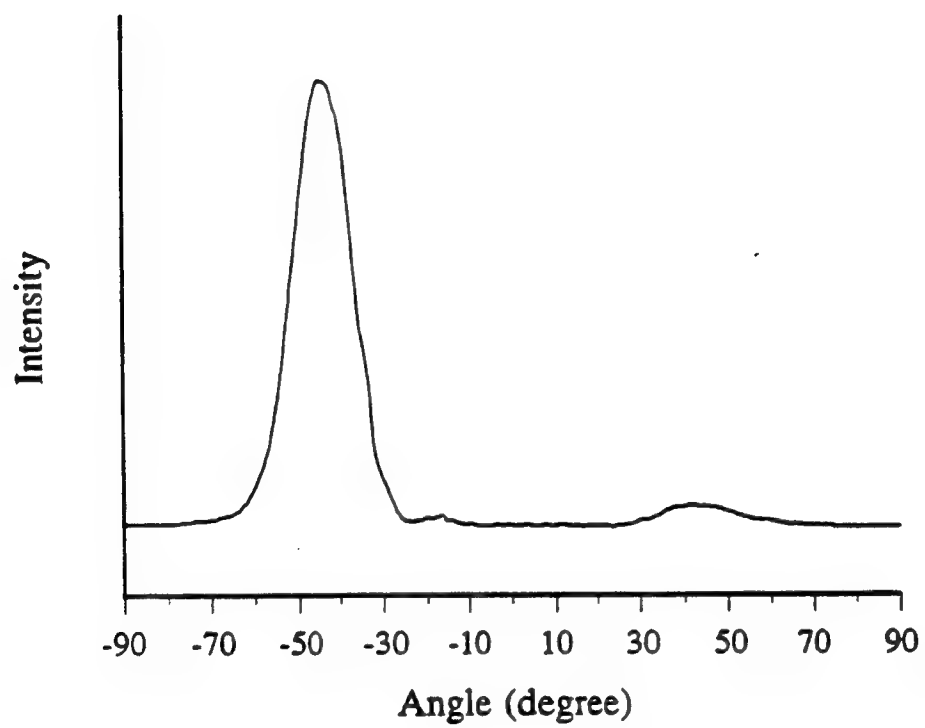
- [1] S.T. Lau, T. Shiraishi, and J.M. Ballantyne, *J. Lightwave Technol.*, LT-12, pp. 202, 1994.
- [2] S. Oku, M. Okayasu, and M. Ikeda, *IEEE Photon. Technol.*, PTL-3, pp. 1066, 1991.
- [3] J.P. Hohimer, G.A. Vawter, and D.C. Craft, *Appl. Phys. Lett.*, vol. 62, pp. 1185, 1993.
- [4] A. Behfar-Rad, S.S. Wong, and J.M. Ballantyne, *Proc. IEDM*, vol. 6(8), pp. 1, 1990.
- [5] J.J. Liang, S.T. Lau, and J.M. Ballantyne, *LEOS'94 Conference Proceedings*, vol. 2, pp. 393, 1994.
- [6] J.J. Liang, and J.M. Ballantyne, *J. Vac. Sci. Technol. B*, vol. 12, pp. 2929, 1994.

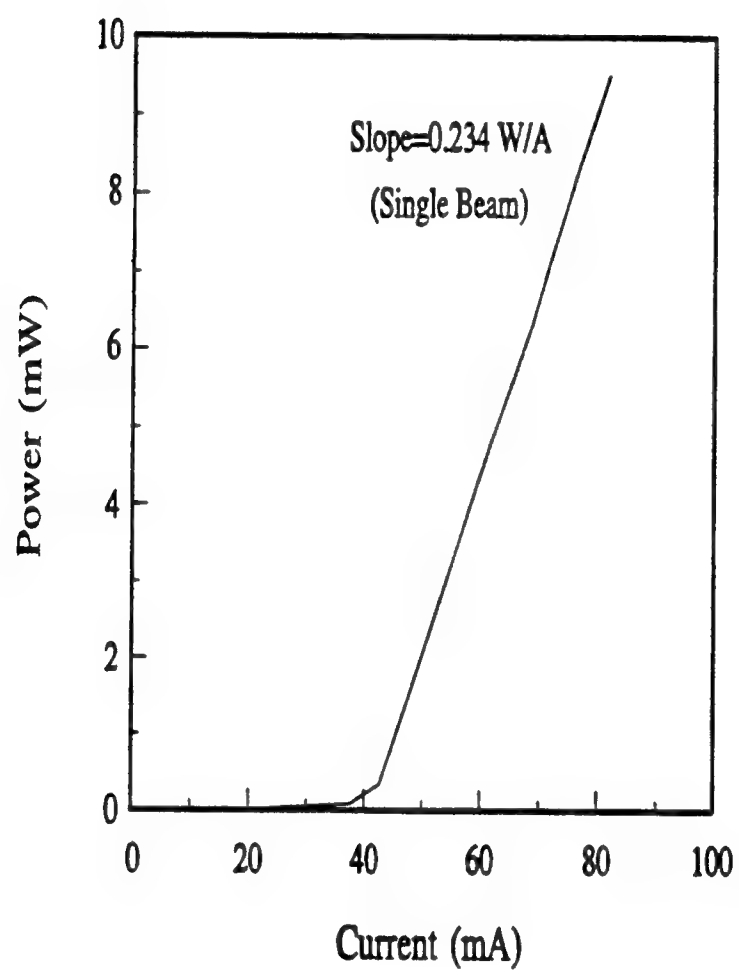
## Figure Captions

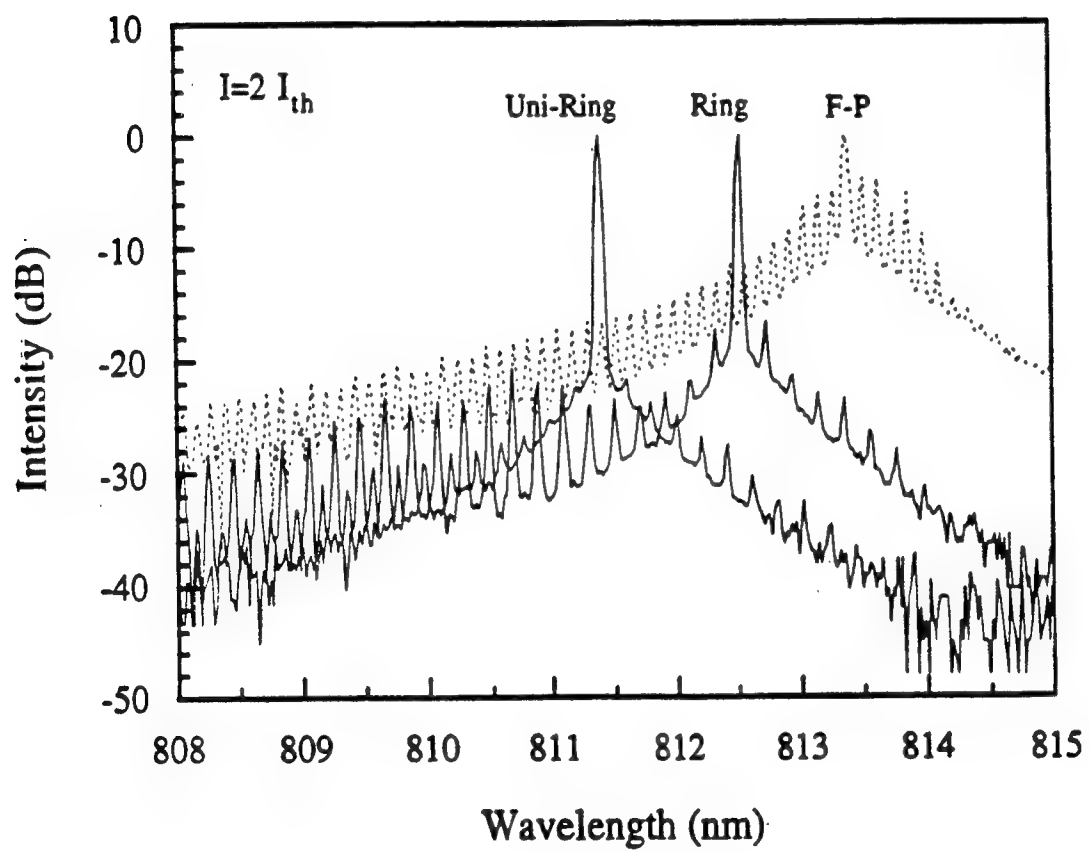
- Fig. 1 SEM of a ring laser with an optical diode.
- Fig. 2 SEM of the tapered waveguide section of a ring laser.
- Fig. 3 The lateral far field of a ring laser with an optical diode.
- Fig. 4 Pulsed single-beam light-current characteristics of a ring laser with an optical diode.
- Fig. 5 CW log-spectra of a unidirectional ring laser with an optical diode, a standard ring laser and a fabry-perot laser, with each laser biased at twice its threshold current.
- Fig. 6 The lateral far field of a ring laser with a tapered waveguide.

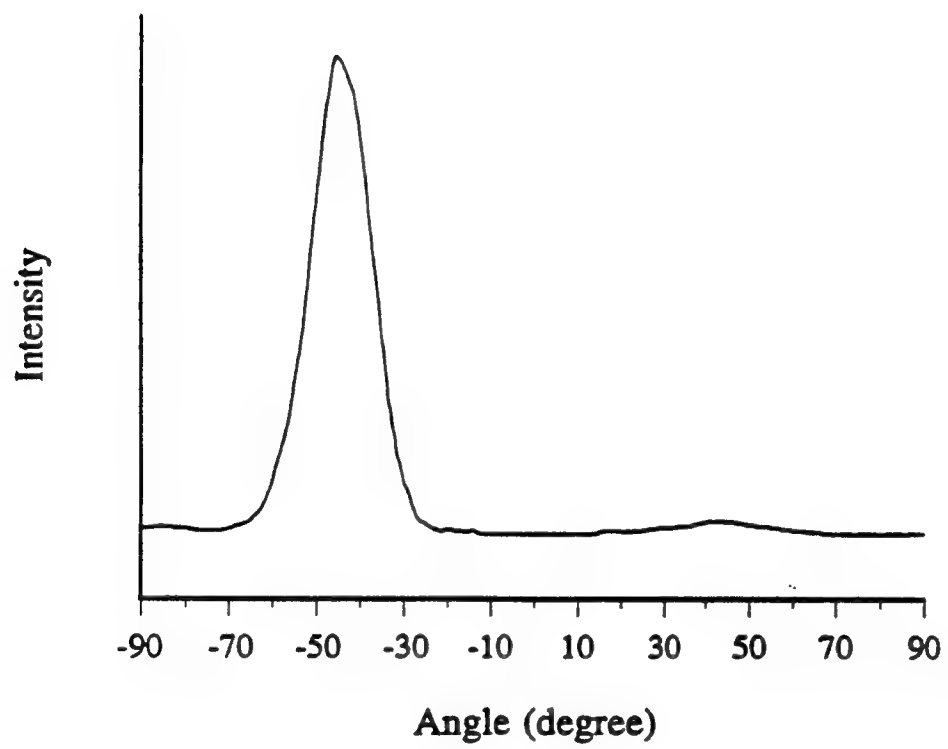














APPENDIX 5

**Monolithic Integration of Tapered Amplifiers with Ring Lasers**

James J. Liang\* and Joseph M. Ballantyne

School of Electrical Engineering,  
Cornell University,  
Ithaca, NY 14853

\*Hewlett-Packard Company, 1040 NE Circle Blvd, Corvallis, OR 97330

**ABSTRACT**

Tapered amplifiers are integrated, for the first time, with semiconductor ring lasers. A Brewster's angle is used for the amplifier output-facet tilt. 85 mW of pulsed output power is achieved with a 600  $\mu\text{m}$  long amplifier.

## Monolithic Integration of Tapered Amplifiers with Ring Lasers

Tapered amplifiers have been intensively investigated, [1-7] in which the amplifier utilizes a tapered lateral waveguide whose angular width is chosen to match the diffraction angle of the input beam, allowing the beam to freely expand as it propagates through the amplifier. While monolithic integration of tapered amplifiers with laser diodes has been demonstrated before, [5-7] this letter reports the first monolithic integration of tapered amplifiers with semiconductor ring lasers.

Shown in Fig. 1 is the SEM of a ring laser integrated with a tapered amplifier. The ring laser was triangular-shaped, with two totally reflecting facets and one output facet. [8, 9] The cavity length, ridge width, and the incidence angle at the output facet for the ring laser was 800  $\mu\text{m}$ , 4  $\mu\text{m}$ , and  $12^\circ$  respectively. The angular spread of the tapered amplifier was chosen to be equal to the diffraction angle of the ring laser beam inside the waveguide, which was determined to be  $5^\circ$ . [9] The amplifier input facet was designed to be parallel to the ring output facet and have the same mirror length as the ring output facet. In order to determine the air gap distance between the ring laser output facet and the amplifier input facet for optimum coupling efficiency into the amplifier, the ring-amplifier interface was approximated as a Fabry-Perot etalon, and the air gap spacing was determined to be 2.7  $\mu\text{m}$  for maximum transmission through the etalon. Of course, this was an over-simplified calculation. A more precise approach which takes into account both the lateral and the transverse directions and the finite extension of both the ring output facet and the amplifier input facet should provide more

optimum design. As shown in Fig.1, a mirror reflector was also implemented in the amplifier structure near the ring output facet facing the counter-clockwise output beam, with the purpose of suppressing the counter-clockwise direction and thus allowing more ring laser power into the amplifier.

Since the amplifier input facet was parallel to the ring output facet, it would have a tilt of  $12^\circ$  with respect to the beam propagation direction. The amplifier output facet was tilted by  $16.8^\circ$  (the Brewster's angle) from the normal with respect to the propagation direction. This Brewster's angle tilt, according to theoretical calculations, [10] would further reduce the back reflection into the cavity as compared to the  $12^\circ$  tilt reported before. [11] The amplifier length was designed to be  $600\text{ }\mu\text{m}$ .

The epitaxial layer was an AlGaAs/GaAs graded index separate confinement heterostructure single quantum well (GRINSCH-SQW) grown by molecular beam epitaxy (MBE), with the quantum well being  $\text{Al}_{0.08}\text{Ga}_{0.94}\text{As}$ . The ring laser-amplifier was fabricated using a self-aligned dry-etching process, [12] with all the mirrors deep etched and the lateral waveguide of both the ring laser and the amplifier shallow etched for single-lateral-mode operation inside the ring laser.

The ring laser-amplifier was tested under pulsed condition (500 ns and 2 KHz). Shown in Fig. 2 is the output power from the ring laser-amplifier as a function of the amplifier current, with the ring laser biased at twice its threshold current. At an amplifier current of 1.2 A, an output power of 85 mW was obtained. Shown in Fig. 3 are the spectral

characteristics of the output from the ring laser-amplifier, with the ring laser biased at 140 mA, and the amplifier biased at 200 mA. The spectrum exhibited a dominant single longitudinal mode, and the mode spacing was found to be 2.15 Å, corresponding to ring operation in an 800  $\mu\text{m}$  cavity.

Shown in Fig. 3 is the lateral far field pattern of the output from the amplifier, with the ring laser biased at 140 mA, and the amplifier biased at 200 mA. The multi-mode pattern of the far field was thought to be due to an oversight in the amplifier design, with the amplifier input facet aligning exactly with the ring output facet. Since the light output angle from the ring is  $42^\circ$ , and the air gap spacing is 2.7  $\mu\text{m}$ , by the time the light reaches the amplifier, the optical mode would already be shifted by about 2.4  $\mu\text{m}$  with respect to the center of the amplifier input facet, which in turn will excite the higher order modes. A new design, in which the amplifier input facet is displaced sideways to compensate for the shift of the mode position, is currently under way.

In conclusion, we have presented the first monolithic integration of ring lasers with amplifiers. A Brewster's angle was used, for the first time, as the amplifier output facet tilt. With an amplifier length of 600  $\mu\text{m}$ , a pulsed output power of 85 mW was achieved from the ring laser-amplifier.

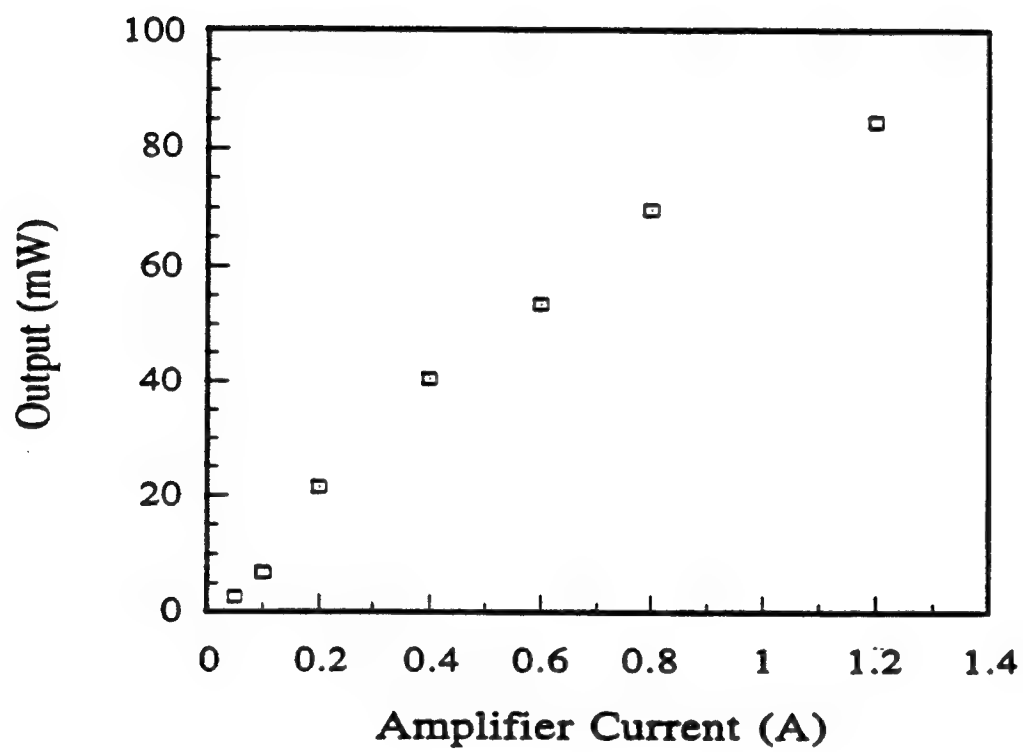
## REFERENCES

- [1] R.R. Craig and P.R. Stephans, *SPIE* 893, 25, 1988.
- [2] G. Bendelli, K. Komori, S. Arai, and Y. Suematsu, *IEEE Photon. Technol. Lett.*, vol. 3, pp. 42, 1991.
- [3] G. Bebdelli, K. Komori, and S. Arai, *IEEE J. Quantum Electron.*, vol. 28, pp. 447, 1992.
- [4] P.A. Yazaki, K. Komori, G. Bebdelli, S. Arai, and Y. Suematsu, *IEEE Photon. Technol. Lett.*, vol. 3, pp. 1060, 1991.
- [5] U. Koren, R.M. Jopson, B.I. Miller, M. Chien, M.G. Young, C.A. Burrus, C.R. Giles, H.M. Presby, G. Raybon, J.D. Evankow, B. Tell, and K. Brown-Goebeler, *Appl. Phys. Lett.*, vol. 59, pp. 2351, 1991.
- [6] D.F. Welch, R. Parke, D. Mehuys, and D. Scifres, *Technical Digest of CLEO's Conference*, Paper No. CWN4, pp. 342-343, 1992.
- [7] D.F. Welch, R. Parke, D. Mehuys, A. Hardy, R. Lang, S. O'Brien, and D. Scifres, *Electron. Lett.*, vol. 28, pp. 2011, 1992.
- [8] A. Behfar-Rad, S.S. Wong, and J.M. Ballantyne, *Proc. IEDM*, vol. 6(8), pp. 1, 1990.
- [9] J.J. Liang, S.T. Lau, and J.M. Ballantyne, *LEOS'94 Conference Proceedings*, vol. 2, pp. 393, 1994.
- [10] S.T. Lau, T. Shiraishi, P.R. McIsaac, A. Behfar-Rad, and J.M. Ballantyne, *J. Lightwave Technol.*, LT-10, pp. 634, 1992.
- [11] C.-F. Lin, *Electron. Lett.*, vol. 27, pp. 96, 1991.
- [12] J.J. Liang, and J.M. Ballantyne, *J. Vac. Sci. Technol. B*, vol. 12, pp. 2929, 1994.

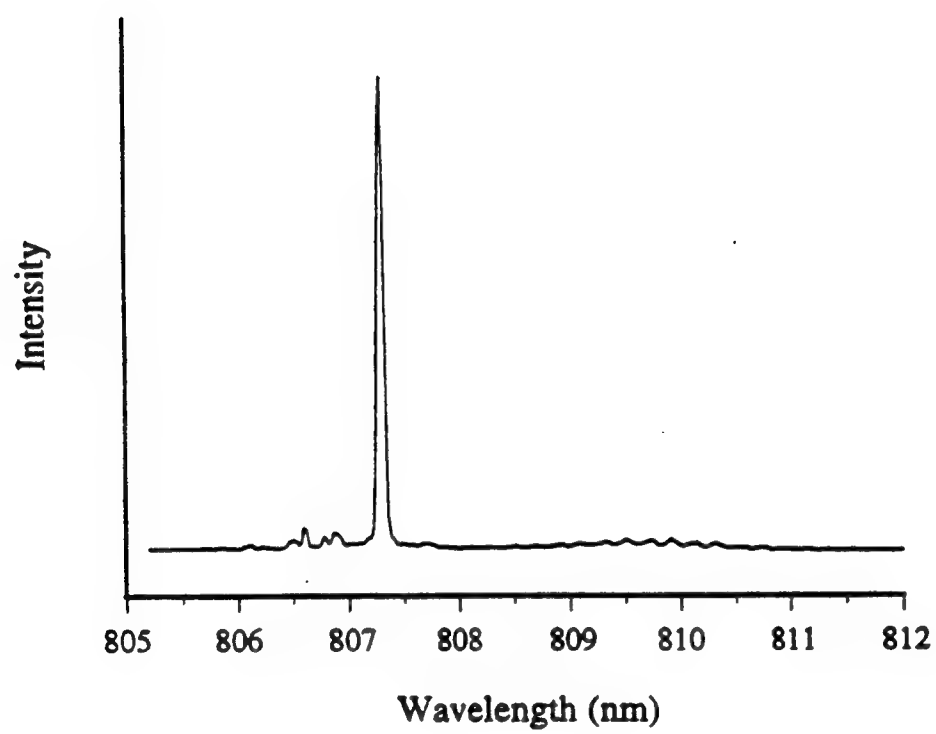
## Figure Captions

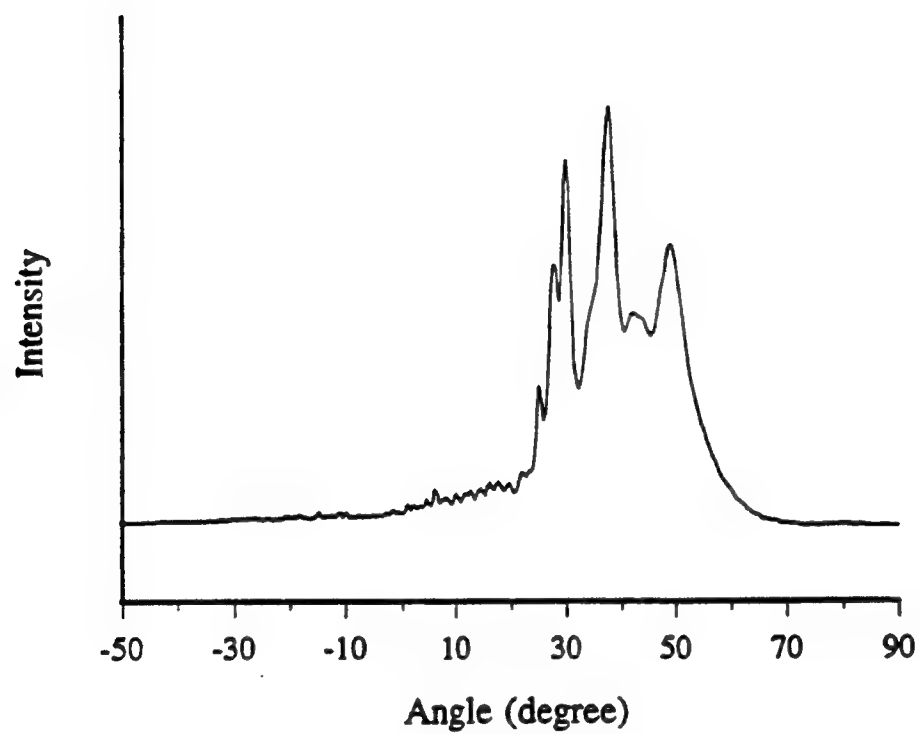
- Fig. 1 SEM of the ring laser integrated with the amplifier.
- Fig. 2 The output power from the ring laser-amplifier as a function of the amplifier current, with the ring laser biased at twice its threshold current.
- Fig. 3 The spectrum of the output from the ring laser-amplifier, at a laser current of 140 mA and an amplifier current of 200 mA.
- Fig. 4 The lateral far field of the output from the amplifier, with a laser current of 140 mA and an amplifier current of 200 mA.











# Method for Control of an Integrated Ring Laser

## APPENDIX 6

### I. Introduction

Ring cavity lasers possess benefits that a Fabry-Perot cavity does not provide. Amongst these is that a unidirectional ring laser will produce lasing action with enhanced mode purity and higher power [Ref]. The difficulty in exploiting this characteristic of ring lasers is to ensure in a deterministic fashion that the laser will indeed be unidirectional, and to be able to control the direction of lasing. The most common, and effective, method currently requires the use of an expensive intra-cavity optical isolator. This device usually has a magnetic medium and utilizes the Faraday Effect to introduce a direction dependent loss. With this nonreciprocal loss, the ring laser will have a preferential direction of lasing. The isolator provides a means of imposing unidirectional operation, however, it requires a magnetic field which adds to the size and cost of the isolator. This method is used for large cavity gas, dye and solid state lasers, however, it cannot be used to control the new generation of integrated ring lasers being currently developed [Ref].

Progress and advances in current monolithic integration technology have allowed lasers of much more complicated geometry to be fabricated, including ring lasers with a variety of cavity configurations [Ref]. These developments expand the prospective applications that integrated semiconductor lasers can be adapted for, and add the attractiveness of size, manufacturability and cost that they provide. The nature of the integrated lasers does not permit the introduction of a conventional optical isolator into the cavity. Therefore, a new method is needed for the control of ring lasers, in particular, a method which can be employed with integrated ring diode lasers. As an additional benefit being able to easily and conveniently switch the lasing direction of the ring laser would be an attractive feature. This paper will present a possible solution to this problem.

It is well known that unwanted retroreflection can have adverse effects on the operation of both Fabry-Perot and ring cavity lasers [Ref]. These reflections are usually caused by

external optics which feed back into the laser cavity producing changes in the output power, spectral character and linewidth of the laser. They can also be intracavity reflections caused by scattering, surface roughness of mirrors, refractive index differences between internal optical components and the laser cavity or, in the case of a diode laser, scattering centers within the semiconductor material. Intra-cavity reflections serve to couple the two possible directions of propagation. This is desirable for a Fabry-Perot laser, and in fact is the basis for the development of the DFB laser. However, it is not desirable for a unidirectional ring laser since this would encourage bidirectional operation. Because of this fact back reflections have always been minimized, even when an optical isolator is employed. However, it has been shown [Ref] that in a ring cavity with unequal back reflections the reflectivity difference is translated into a difference in the powers of the oppositely circulating waves, and hence a difference in the output powers of the two directions of the ring laser. This asymmetric cross coupling of the two directions of propagation has been proven to produce unidirectional lasers [Ref]. This fact will be exploited to control the direction of lasing of a ring laser.

Ring laser operation is very sensitive to the differences in the back reflectivity at any of the components of the cavity [Ref], and depending on the actual difference the relative ratio of the two output beams can be very large. Therefore, the direction of lasing can be controlled by adjusting the relative back reflectivities so that one or the other direction contains the dominant power. It should be noted that the theory does not predict the complete extinction of one of the beams, only that one power can be made much larger than the other, thus an essentially unidirectional mode of operation is achieved.

This paper will discuss a method for deterministically creating a variable back reflectivity difference (an asymmetric reflector) in order to control the lasing direction of a ring laser.

## **II. The Asymmetric Reflector**

There are a variety of possible ways to create an asymmetric cross coupling of the directions of propagation in a ring laser. These include the use of a cross over waveguide [Ref], asymmetric saturable absorber regions [Ref] and asymmetric reflectors. This paper is more concerned with the creation of an asymmetric reflector (i.e. a region which produces different reflection

coefficients depending on the direction of incidence). Examples of these are asymmetric index profiles, for example, a graded index profile for one direction and an abrupt profile for the other. Or a physically asymmetric transition, one which is gradual on one side and abrupt on the other. Unfortunately, both of these methods while creating an asymmetric reflector do not allow the direction of lasing to be actively changed since the features are permanent. To avoid these nonchangeable structures the proposed asymmetric reflector can be obtained through the use of a reflector stack with material which has a complex material impedance (the imaginary part is due to loss or gain), that is an active material.

Fig. 1 shows a triangular ring laser (this geometry is chosen only for illustration purposes, any ring cavity may be used) with the proposed design for the asymmetric reflector. It is a simple four layer structure with the first and last layers assumed to be the same material, however, no assumptions are made about the type of materials used and all impedances can be complex.

As a first approximation, the concept of the asymmetric reflector will be described using the structure in Fig. 1 and a simple plane wave approach. This is a rather simple model and in reality things will be more complicated, but this is sufficient to convey the idea behind the formation of the asymmetric reflector and the control of the back reflectivities. Only normal incidence is considered here since this is the most likely mode of operation (extension to oblique incidence is a simple matter which only complicates the presentation without providing further insight).

Using the plane wave approach and techniques described in most introductory electromagnetic theory books [Ref], the reflectivity from the left and right sides of Fig. 1, respectively, are

$$\Gamma_L = \frac{\eta_2(\eta_3^2 - \eta_1^2)C_2S_3 + \eta_3(\eta_2^2 - \eta_1^2)S_2C_3 + \eta_1(\eta_2^2 - \eta_3^2)S_2S_3}{D} \quad (1)$$

$$\Gamma_R = \frac{\eta_2(\eta_3^2 - \eta_1^2)C_2S_3 + \eta_3(\eta_2^2 - \eta_1^2)S_2C_3 - \eta_1(\eta_2^2 - \eta_3^2)S_2S_3}{D} \quad (2)$$

$$D = \eta_3(\eta_2^2 + \eta_1^2)S_2C_3 + 2\eta_1\eta_2\eta_3C_2C_3 + \eta_1(\eta_2^2 + \eta_3^2)S_2S_3 + \eta_2(\eta_1^2 + \eta_3^2)C_2S_3 \quad (3)$$

$$\eta_i = \frac{\omega\mu_i}{\alpha_i^2 + k_i^2}(k_i + j\alpha_i) \quad (4)$$

$$C_i = \cosh((\alpha_i + jk_i)d_i) = \cosh(\alpha_id_i)\cos(k_id_i) + j\sinh(\alpha_id_i)\sin(k_id_i) \quad (5)$$

$$S_i = \sinh((\alpha_i + jk_i)d_i) = \sinh(\alpha_id_i)\cos(k_id_i) + j\cosh(\alpha_id_i)\sin(k_id_i) \quad (6)$$

Where the complex propagation constant for material “i” is  $\tilde{k}_i = k_i - j\alpha_i$ .  $k_i$  is for the phase accumulation and  $\alpha_i$  represents the gain coefficient (positive for gain and negative for loss).

For the purpose of this discussion, although the expression for the denominator of  $\Gamma_L$  and  $\Gamma_R$  is given in Equation (3), it is enough to know that it is the same for both coefficients. It is the functional difference of the reflection coefficients that is really important. The only difference between Equations (1) and (2) (i.e.  $\Gamma_L$  and  $\Gamma_R$ ) is the third term in the numerator, and there is only a sign difference here. However, the key to this design is the fact that  $C_i$ ,  $S_i$  and  $\eta_i$  are all complex. Taking this into account then the sign difference of the third term is all that is needed to make  $|\Gamma_L| \neq |\Gamma_R|$ . Therefore, a different fraction of the incident power (i.e.  $|\Gamma|^2$ ) is reflected depending on the incidence direction. This term also shows that  $\eta_2$  must not be the same as  $\eta_3$ , else the reflectivities will be the same (since this term goes to zero). This condition simply enforces the fact that there must be an asymmetry in the stack for an asymmetry in the back reflectivities to exist.

Another condition for asymmetric reflectivities is that at least one of the materials must have a complex impedance (i.e. there must be gain or loss somewhere within the stack). If all of the materials are lossless then the first and second terms in the numerator will be purely imaginary and the third purely real. For this case then  $|\Gamma_L| = |\Gamma_R|$  and the power reflection coefficients are the same.

It is easy to verify that the transmission coefficients are

$$T_{LR} = T_{RL} = \frac{2\eta_1\eta_2\eta_3}{D} \quad (7)$$

for incidence from the left and right of Fig. 1. This equation shows that the reciprocity of the stack is maintained (same power transmission  $|T|^2$ ), as expected.

It is evident from the above discussion that an asymmetric reflector can be made controllable by adjusting either the refractive indices of the materials or by changing the gain or loss in each section. As an example, control of the reflectivity difference may be achieved dynamically by the use of the electro-optic effect, whereby the refractive indices can be adjusted by the application of an electric field. The change in index is proportional to the applied field, so by using various field strengths the reflectivity difference can be controlled.

For diode lasers, another simple option is available. Multiple contacts can be placed close together and the gain of each section changed by varying the current to that section. This would provide an extremely easy way of switching the lasing direction by simply changing the currents to the respective sections.

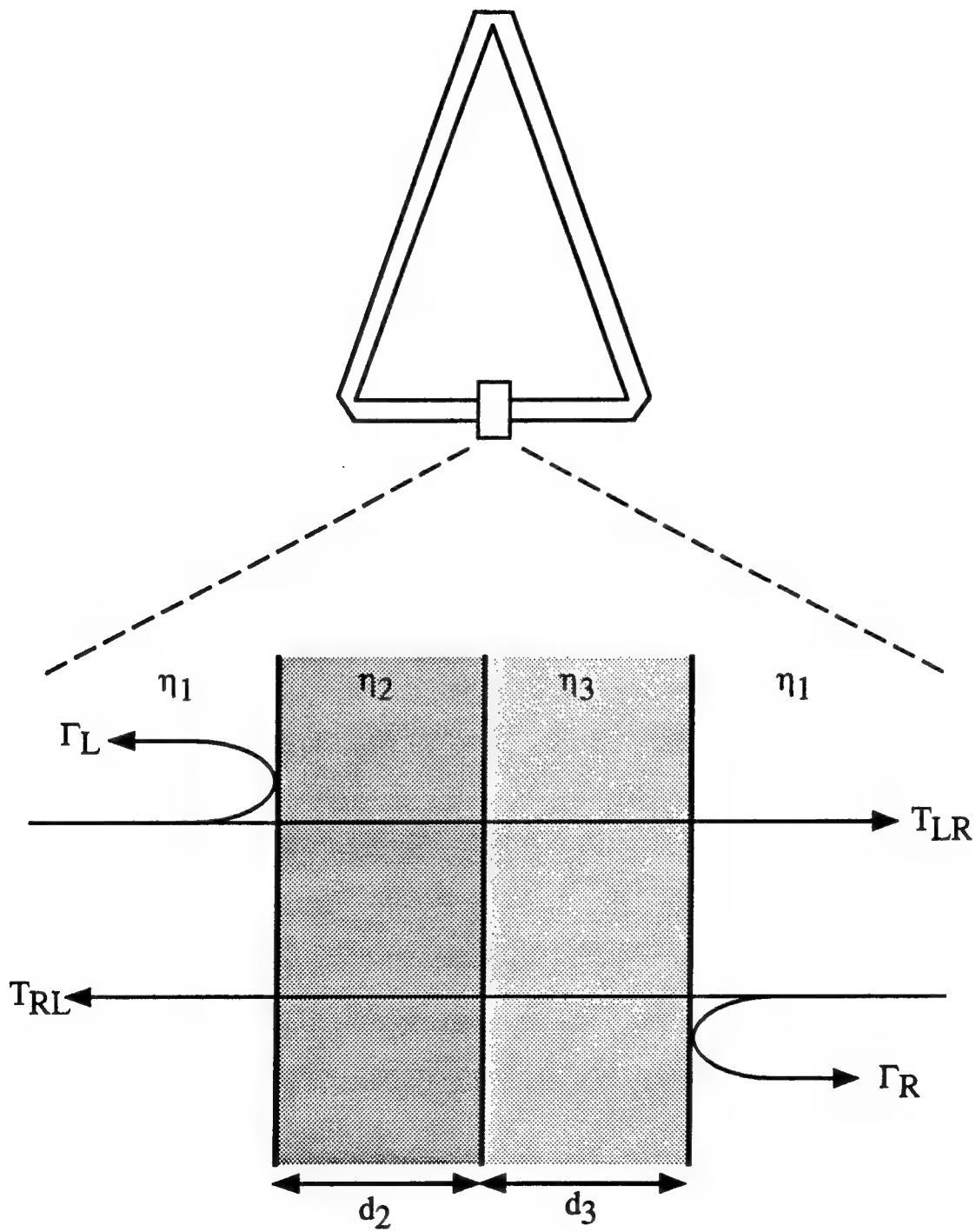
In Fig. 1 the reflector stack is depicted as being in a symmetric position within the laser cavity. However, due to phase and gain considerations the position of the reflector stack within the cavity will also influence the overall performance of the laser [Ref] and must be accounted for in the laser cavity design.

To employ the asymmetric reflector, as proposed, in a laser cavity it will be necessary to maximize the transmission while at the same time maximizing the difference in the reflectivities. This is necessary to reduce the losses of the cavity. These two goals may not be compatible and some trade off between the laser threshold and the degree of unidirectionality may have to be tolerated. Fortunately, this may not be a real concern since an active medium with gain can be used to provide the desired complex impedance needed for the reflector to work.

The analysis here is not meant to be comprehensive, and can easily be generalized, particularly for the case of more layers in the reflector stack. However, the general comments are still valid. To create an asymmetric reflector the stack must be asymmetric and at least one of the materials must have complex impedance.

### III. Conclusion

This asymmetric reflector design coupled with ring cavity theory indicates that an essentially unidirectional laser can be formed without the use of optical isolators. The method described here is more easily applied for use with integrated diode ring lasers for controlling their direction of oscillation. However, the basic concept can be applied to other types of ring lasers. The elimination of the need for optical isolators to achieve unidirectional operation of ring lasers may greatly reduce the cost of these lasers while still maintaining the benefits that they provide. In addition, the introduction of mass produceable integrated lasers could greatly expand the use of ring lasers in many diverse applications.





# DISTRIBUTION LIST

addresses	number of copies
ROME LABORATORY/OCPC ATTN: PAUL L. REPAK 25 ELECTRONIC PKY ROME NY 13441-4515	5
CORNELL UNIVERSITY OFFICE OF SPONSORED PROGRAMS 120 DAY HALL ITHACA NY 14853	5
ROME LABORATORY/SUL TECHNICAL LIBRARY 26 ELECTRONIC PKY ROME NY 13441-4514	1
ATTENTION: DTIC-OCC DEFENSE TECHNICAL INFO CENTER 8725 JOHN J. KINGMAN ROAD, STE 0944 FT. BELVOIR, VA 22060-6218	2
ADVANCED RESEARCH PROJECTS AGENCY 3701 NORTH FAIRFAX DRIVE ARLINGTON VA 22203-1714	1
NAVAL WARFARE ASSESSMENT CENTER GIDEP (QA50) ATTN: RAYMOND TADROS PO BOX 3000 CORONA CA 91718-8000	1
WRIGHT LABORATORY/AAAI-2, BLDG 635 2185 AVIONICS CIRCLE WRIGHT-PATTERSON AFB OH 45433-7301	1
AFIT ACADEMIC LIBRARY/LDEE 2950 P STREET AREA B, BLDG 642 WRIGHT-PATTERSON AFB OH 45433-7765	1

WRIGHT LABORATORY/MLPO 1  
ATTN: R. L. DENISON  
BLDG 651  
3005 P STREET, STE 6  
WRIGHT-PATTERSON AFB OH 45433-7707

WRIGHT LABORATORY/MTE, BLDG 653 1  
2977 P STREET, STE 6  
WRIGHT-PATTERSON AFB OH 45433-7739

AL/CFHI, BLDG 248 1  
ATTN: GILBERT G. KUPERMAN  
2255 H STREET  
WRIGHT-PATTERSON AFB OH 45433-7022

AIR FORCE HUMAN RESOURCES LAB 1  
TECHNICAL DOCUMENTS CENTER  
OL AL HSC/HRG, BLDG 190  
WRIGHT-PATTERSON AFB OH 45433-7604

AUL/LSE 1  
BLDG 1405  
600 CHENNAULT CIRCLE  
MAXWELL AFB AL 361126424

US ARMY SPACE & STRATEGIC 1  
DEFENSE COMMAND  
CSSD-IM-PA  
PO BOX 1500  
HUNTSVILLE AL 35897-3801

NAVAL AIR WARFARE CENTER 1  
6000 E. 21ST STREET  
INDIANAPOLIS IN 46219-2189

COMMANDING OFFICER 1  
NCCOSC RDTE DIVISION  
ATTN: TECHNICAL LIBRARY, CODE 0274  
53560 HULL STREET  
SAN DIEGO CA 92152-5001

COMMANDER, TECHNICAL LIBRARY 1  
474700D/C0223  
NAVAIRWARCENWPNDIV  
1 ADMINISTRATION CIRCLE  
CHINA LAKE CA 93555-6001

SPACE & NAVAL WARFARE SYSTEMS  
COMMAND (PMW 178-1)  
2451 CRYSTAL DRIVE  
ARLINGTON VA 22245-5200

2

SPACE & NAVAL WARFARE SYSTEMS  
COMMAND, EXECUTIVE DIRECTOR (PD804)  
ATTN: MR. CARL ANDRIANI  
2451 CRYSTAL DRIVE  
ARLINGTON VA 22245-5200

1

COMMANDER, SPACE & NAVAL WARFARE  
SYSTEMS COMMAND (CODE 32)  
2451 CRYSTAL DRIVE  
ARLINGTON VA 22245-5200

1

US ARMY MISSILE COMMAND  
AMSMI-PD-CS-R/DOCUMENTS  
RSIC BLDG 4484  
REDSTONE ARSENAL AL 35898-5241

2

ADVISORY GROUP ON ELECTRON DEVICES  
1745 JEFFERSON DAVIS HWY  
SUITE 500  
ARLINGTON VA 22202

1

LOS ALAMOS NATIONAL LABORATORY  
PO BOX 1663  
REPORT LIBRARY, P364  
LOS ALAMOS NM 87545

1

AEDC LIBRARY  
TECHNICAL REPORTS FILE  
100 KINDEL DRIVE, SUITE C211  
ARNOLD AFB TN 37389-3211

1

COMMANDER  
USAISC  
ASHC-IMD-L, BLDG 61801  
FT HUACHUCA AZ 85613-5000

1

US DEPT OF TRANSPORTATION LIBRARY  
FB104, M-457, RM 930  
800 INDEPENDENCE AVE, SW  
WASH DC 22591

1

AFIWC/MSO  
102 HALL BLVD, STE 315  
SAN ANTONIO TX 78243-7016

1

DIRNSA  
R509  
9800 SAVAGE ROAD  
FT MEADE MD 20755-6000

1

NSA/CSS  
K1  
FT MEADE MD 20755-6000

1

PHILLIPS LABORATORY  
PL/TL (LIBRARY)  
5 WRIGHT STREET  
HANSCOM AFB MA 01731-3004

1

THE MITRE CORPORATION  
ATTN: E. LADURE  
D460  
202 BURLINGTON RD  
BEDFORD MA 01732

1

OUSD(P)/DTSA/DUTD  
ATTN: PATRICK G. SULLIVAN, JR.  
400 ARMY NAVY DRIVE  
SUITE 300  
ARLINGTON VA 22202

2

ROME LABORATORY/ERAA  
ATTN: DAVID D. CURTIS  
HANSCOM AFB, MA 01731-5000

1

ROME LABORATORY/ERO  
ATTN: RICHARD PAYNE  
HANSCOM AFB, MA 01731-5000

1

ROME LABORATORY/EROC  
ATTN: JOSEPH P. LORENZO, JR.  
HANSCOM AFB, MA 01731-5000

1

ROME LABORATORY/EROP  
ATTN: JOSEPH L. HORNER  
HANSCOM AFB, MA 01731-5000

1

ROME LABORATORY/EROC  
ATTN: RICHARD A. SOREF  
HANSCOM AFB, MA 01731-5000

1

ROME LABORATORY/ERXE  
ATTN: JOHN J. LARKIN  
HANSCOM AFB, MA 01731-5000

1

ROME LABORATORY/ERDR  
ATTN: DANIEL J. BURNS  
525 BROOKS RD  
ROME NY 13441-4505

1

ROME LABORATORY/IRAP  
ATTN: ALBERT A. JAMBERDINO  
32 HANGAR RD  
ROME NY 13441-4114

1

ROME LABORATORY/OCP  
ATTN: BRIAN M. HENDRICKSON  
25 ELECTRONIC PKY  
ROME NY 13441-4515

1

ROME LABORATORY/OCPC  
ATTN: GREGORY J. ZAGAR  
25 ELECTRONIC PKY  
ROME NY 13441-4515

1

ROME LABORATORY/C3BC  
ATTN: ROBERT L. KAMINSKI  
525 BROOKS RD  
ROME NY 13441-4505

1

ROME LABORATORY/OCP  
ATTN: JAMES W. CUSACK  
25 ELECTRONIC PKY  
ROME NY 13441-4515

1

ROME LABORATORY/OCP  
ATTN: JOANNE L. ROSSI  
25 ELECTRONIC PKY  
ROME NY 13441-4515

1

ROME LABORATORY/OCPA  
ATTN: ANDREW R. PIRICH  
25 ELECTRONIC PKY  
ROME NY 13441-4515

1

ROME LABORTORY/OCP  
ATTN: RICHARD J. MICHALAK  
25 ELECTRONIC PKY  
ROME NY 13441-4515

1

NY PHOTONIC DEVELOPMENT CORP  
MVCC ROME CAMPUS  
UPPER FLOYD AVE  
ROME, NY 13440

1

NRAD/CODE 55  
ATTN: DR. STEVE PAPPERT  
SAN DIEGO CA 92152-5000

1

PHILLIPS LABORATORY/VTET  
ATTN: MR. EDWARD W. TAYLOR  
3550 ABERDEEN AVENUE SE, BLDG 902  
KIRTLAND AFB NM 87117-5776

1

LABORATORY FOR PHYSICAL SCIENCES  
ATTN: DONALD LA FAY  
4928 COLLEGE AVENUE  
COLLEGE PARK MD 20740

1

WRIGHT LABORATORY/XPN  
ATTN: E. UTT  
BLDG 254  
2591 "K" STREET  
WRIGHT-PATTERSON AFB OH 45433-7602

1

***MISSION  
OF  
ROME LABORATORY***

Mission. The mission of Rome Laboratory is to advance the science and technologies of command, control, communications and intelligence and to transition them into systems to meet customer needs. To achieve this, Rome Lab:

- a. Conducts vigorous research, development and test programs in all applicable technologies;
- b. Transitions technology to current and future systems to improve operational capability, readiness, and supportability;
- c. Provides a full range of technical support to Air Force Materiel Command product centers and other Air Force organizations;
- d. Promotes transfer of technology to the private sector;
- e. Maintains leading edge technological expertise in the areas of surveillance, communications, command and control, intelligence, reliability science, electro-magnetic technology, photonics, signal processing, and computational science.

The thrust areas of technical competence include: Surveillance, Communications, Command and Control, Intelligence, Signal Processing, Computer Science and Technology, Electromagnetic Technology, Photonics and Reliability Sciences.